INVESTIGATION OF POLYACRYLIC ACID BASED TERPOLYMER COATINGS

A **Major Project**

Submitted for the partial fulfilment of the award for the

Degree of

Master of Technology

In

Polymer Technology

Under the supervision of

Dr. Archna Rani

Submitted by

Navneet Kumar

(Roll No: 2K12/PTE/07)

DEPARTMENT OF APPLIED CHEMISTRY AND POLYMER TECHNOLOGY

DELHI TECHNOLOGICAL UNIVERSITY

Delhi-110042

July-2014

CERTIFICATE

I hereby certify that the work which is being presented in the thesis entitled "**INVESTIGATION OF POLYACRYLIC ACID BASED TERPOLYMER COATINGS"** for the partial fulfilment of the award of degree of **MASTER OF TECHNOLOGY** at **DELHI TECHNOLOGICAL UNIVERSITY, DELHI**, is an authenticated record of NAVNEET KUMAR submitted in the Department Of Applied Chemistry And Polymer Technology carried out during 4TH semester, under my supervision.

Dr. Archna Rani   **Prof. Dr. D. KUMAR**
Project Guide   **Head of Department**
Dept. of Applied Chemistry   Dept. of Applied Chemistry
& Polymer Technology, DTU   & Polymer Technology, DTU

Declaration

I Navneet Kumar, hereby certify that the work presented in the thesis is original, results are not copied from anywhere else and the experiments were carried out at Department of Applied chemistry and polymer technology.

Navneet Kumar

M.Tech (Polymer technology)

2k12/PTE/07

ACKNOWLEDGEMENT

Navneet Kumar

M.Tech (Polymer Technology)

Roll No. 2K12/PTE/07

<u>CONTENTS</u>

List of figures

<u>List of tables</u>

Coding and Abbreviations

1.	**PAA**	**P**oly**a**crylic **a**cid
2.	**ASM**	**A**crylic acid-**s**tyrene-**m**aleic anhydride
3.	**ASM52**	**ASM** with **5** % styrene, **2**% maleic anhydride by weight
4.	**ASM102**	**ASM** with **10**% styrene, **2**% maleic anhydride by weight
5.	**ASM73**	**ASM** with **7** % styrene, **3**% maleic anhydride by weight
6.	**ASM74**	**ASM** with **7** % styrene, **4**% maleic anhydride by weight
7.	**ASM73 C**	**ASM** with **7** % styrene, **3**% maleic anhydride **C**omposite by weight
8.	**ASM74 C**	**ASM** with**7** % styrene, **4**% maleic anhydride **C**omposite by weight
9.	**PAA-G**	**PAA** coated **g**lass

ABSTRACT

In the current piece of work, Polyacrylic acid based terpolymers; **A**crylic acid-**S**tyrene-**M**aleic anhydride (**ASM**); were synthesized with different percentage by weight of **S**tyrene and **M**aleic anhydride viz. **ASM52** (**5** % styrene, **2**% maleic anhydride), **ASM102** (**10** % styrene, **2**% maleic anhydride), **ASM73** (**7** % styrene, **3**% maleic anhydride) and **ASM74** (**7** % styrene, **4**% maleic anhydride) following bulk polymerization. The composites of **ASM73** and **ASM74 (ASM73 C** and **ASM74 C)** were also developed using TiO_2-Al_2O_3. The samples were characterized using Fourier transform infrared (FTIR) spectroscopy (for functional groups and to confirm the chemical interaction between TiO_2-Al_2O_3 and organic moiety) and Energy Dispersive x-ray Spectroscopy (EDS) for elemental analysis. Thermal analysis revealed that no physical or chemical changes took place upto130^o C in **ASM73 C** and 138° C in **ASM74 C.** The samples were investigated to evaluate their potentiality as coating material for glass. Thus, mechanical properties of terpolymer coated glass (**ASM52-G , ASM102-G, ASM73-G** and **ASM74-G**) and composite coated glass (**ASM73 C-G** and **ASM74 C-G**) ; in terms of flexural and Izod impact strength; was determined and compared with that of the normal glass and **P**oly **A**crylic **A**cid coated glass(**PAA-G**). **ASM73 C-G** and **ASM74 C-G** were found to have unexpectedly high flexural strengths (146.20 and 136.01 MPa respectively) as compared to uncoated glass (68.75MPa), **PAA-G** (85.96 MPa) and glass coated with different samples of terpolymers synthesized during current investigation. Similarly the impact strengths of **ASM73 C-G** and **ASM74 C-G;** 43.33 and 40 j/m respectively; are remarkably higher than that of glass (22.85 j/m) and **PAA-G** (26.66 j/m). Surface morphology of the coatings was studied by using Scanning electron microscopy (SEM). It was observed that the mechanical strength of **ASM73C-G** and **ASM74 C-G** are comparable but **ASM74 C-G** possesses better clarity thus can be used where transparency is highly desirable**.** Also the coatings prevented the broken glass pieces from shattering which makes the glass safer for indoor applications.

CHAPTER 1   INTRODUCTION

1.1 Background

Polyacrylic acid was patented in 1966 by Gene Harper of Dow Chemical and Carlyle Harmon of Johnson & Johnson [1]. It was first used in diapers in 1982 in Japan. The sodium and ammonium salts have been used as emulsion-thickening agents, in particular for rubber latex. The polymers derived from the esters of acrylic acid are used as a base in many paints and varnishes. About 50% of the acrylic acid is used to make esters, mainly methyl, ethyl and butyl propenoates. These are, in turn, polymerized. About 30% is used to make Polyacrylic acid. Annual production of Acrylic acid in World   is 1.8 million tonnes and in Europe is 380,000 tonnes. Polyacry1ic acid (Figure 1) is insoluble in its monomer but soluble in water. It does not become thermoplastic when heated.
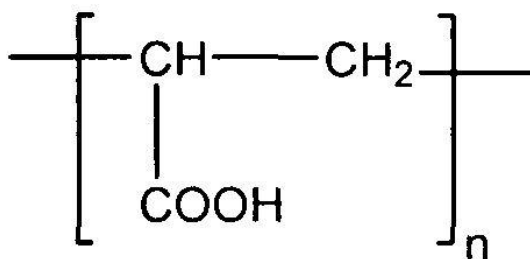
Figure 1: Structure of Polyacry1ic acid

Acrylic acid, the monomer of polyacrylic acid is prepared from propene by two step oxidation process. It possesses extreme water absorption because of the ionic nature. Also it interacts with a wide variety of metal ions (e.g. adhesion to metal substrates such as copper, zinc, aluminium). Because of its hydrophilic nature polyacrylic acid is widely used to modify the rheological properties and used for pharmaceutical purposes. One of the famous examples is Carbopol [2]. Carbopol polymers are polymers of acrylic acid cross-linked with polyalkenyl ethers or divinyl glycol. They are readily water-swellable. Carbopol polymers are used in a diverse range of pharmaceutical applications.

Carbopol polymers offer consistent performance over a wide range of desired parameters. Although Carbopol polymers have enjoyed success in controlled-release solid dose formulations since the 1960s, the number of companies developing and commercializing controlled-release tablets using Carbopol polymers has increased significantly in recent years. Other areas of applications of polyacrylic acid are nanotechnology, lithography, textile (carpets, leather), water treatment (flocculants), paints, cosmetics and Personal care and thermoplastics (shoes, glass, metals, cables and wires, insulation, adhesives) etc.

Though the hydrophilic nature of polyacrylic acid makes it useful but its water solubility limits its applications. For applications in which water resistance is required, it is usually copolymerized with maleic anhydride to increase its water resistance. Maleic anhydride act as cross-linking agent and use of 5 mol % of Maleic anhydride makes the polymer insoluble in water[3]. Copolymers of acrylic acid with styrene (Figure 2) are also present and the bulky phenyl ring of styrene improves mechanical properties of the copolymer. Thus Styrene and maleic anhydride together can balance the properties of the polymer formed with acrylic acid. It gives a reason to synthesize the terpolymer in the current investigation.
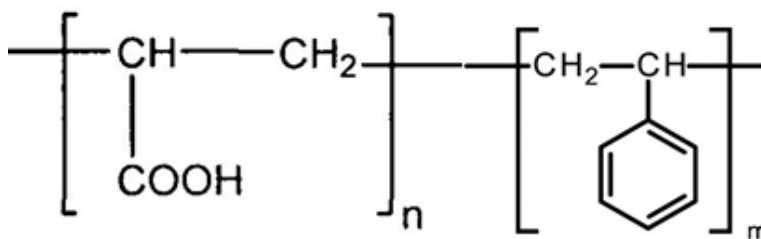
Figure 2: Structure of Acrylic acid-Styrene copolymer

Composites of polyacrylic acid are also common. A wide range of composites of polyacrylic acid with nanoparticles are present. The commonly used nanoparticles with polyacrylic acid are

I.   Titanium Dioxide (TiO_2)
II. Alumina (Al_2O_3)
III. Silica (SiO_2)
IV. Zinc Oxide (ZnO)

Polyacrylic acid forms stable composite with the above particulate reinforcements. Generally polyacrylic acid is used to modify the surface of the nanoparticles for better surface properties. Due to their extremely large surface-area/particle-size ratio, nanoparticles tend to strongly agglomerate, hence reducing the resultant mechanical properties of the nanocomposite materials. Compatibility between the particle and the polymer matrix is important for a composite and compatibility of polyacrylic acid matrix with metallic nanoparticles is mainly due the presence of the carboxylic functional group. This carboxylic acid gives polyacrylic acid the ability to interact with metals. This fact is used in making absorbents for absorption of metals from aqueous solutions. At present, researches are going on for the development of detectors based on polyacrylic acid and its copolymers with styrene, maleic anhydride, acrylamide and polyaniline. Polyacrylic acid is used as coatings because of its good adhesion strength, transparency but PAA coating suffers from low mechanical strength and water solubility. The mechanical strength of the PAA coated glass can be increased by copolymerization and use of reinforcements. The development of terpolymer composite of acrylic acid with particulate reinforcement is not reported yet. Keeping this point in mind, we initiated the current investigation with the following objectives.

1.2 OBJECTIVE

Polyacrylic acid has the potential to be used as coating for glass. The objective of this project is to develop a terpolymer (Figure 3) of acrylic acid with styrene and maleic anhydride and composites of this terpolymer with $TiO_2 - Al_2O_3$ which can be used as protective coating for glass respectively. The comonomer styrene was selected because of its ability to impart toughness which can improve the flexural strength and impact strength of the coating. Maleic anhydride was used as second comonomer because of its ability to cross link which can decrease the solubility of terpolymer in water. Titanium dioxide (TiO_2) was used to enhance its mechanical strength. Alumina (Al_2O_3) was used with Titanium dioxide (TiO_2) for the prevention of free radical generation which decreases the rate of the polymer degradation.
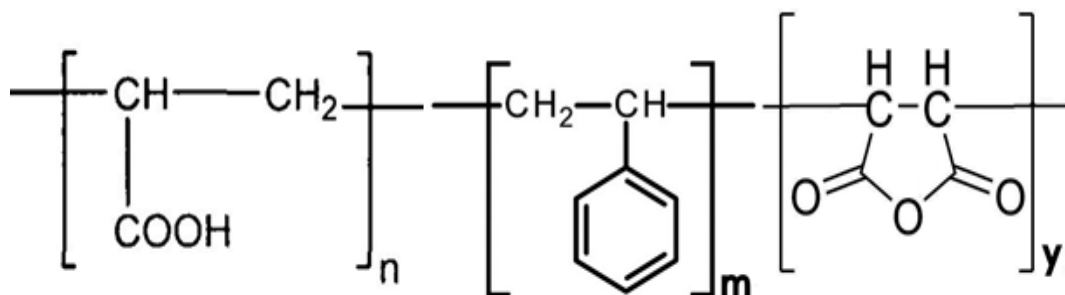
Figure 3: Poly(acrylic acid-styrene-maleic anhydride) terpolymer

Poly(acrylic acid-styrene-maleic anhydride) terpolymer was developed and their properties were evaluated. The mechanical properties were investigated using flexural strength test and Izod impact test. The samples were also characterized using FTIR spectroscopy and EDS. Izod impact test and flexural test showed that there is significant increase in the flexural and impact strength. The **ASM73 C-G** and **ASM74 C-G** exhibited best mechanical strength; they showed a remarkable increase in the flexural and the impact strength. This increase in the flexural and impact strength is due to the introduction of the comonomers styrene and maleic anhydride and reinforcement with $TiO_2-Al_2O_3$. This terpolymer and composites with better mechanical properties can be used in applications which require good impact and flexural strength.

14

CHAPTER 2   <u>**LITERATURE REVIEW**</u>

Polyacrylic acid has a wide range of applications and researchers have shown a lot of interest in the development of its copolymers, terpolymers and composites. Styrene, maleic anhydride and acrylonitrile were commonly used with acrylic acid to modify its properties according to the application. Use of vinyl alcohol with acrylic acid is also very common because both are hydrophilic in nature. Polyacrylic acid is widely used in biomedical applications.

2.1 Copolymers of Acrylic acid

For the past many years, Copolymers of acrylic acid attracted the interest of scientists worldwide due to the widespread applications. Yun-ren Qiu et al developed copolymer of acrylic acid and maleic acid for removal of manganese from waste water by complexation−ultrafiltration[4]. The Copolymer (Figure 4) of acrylic acid and maleic acid (PMA-100), combining with polyvinyl butyral (PVB) ultrafiltration membrane was used for the removal of Mn(II) from waste water by complexation−ultrafiltration. The carboxylic group content of PMA-100 and the rate of complexation reaction were measured. The results showed that carboxylic group content of PMA-100 is 9.5 mmol/g. The complexation of Mn(II) with PMA-100 is rapid and completed within 5 min at pH 6.0.
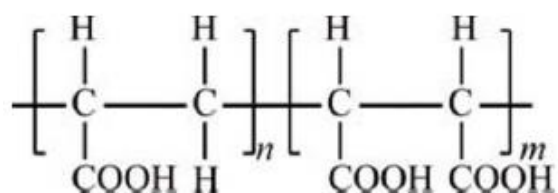
Figure 4: Structure of PMA-100

J.L. de la Fuente et al prepared poly(acrylic acid-g-styrene) amphiphilic graft copolymers and performed thermal, morphological and rheological characterization[5]. In their experiment they prepared a family of amphiphilic poly(acrylic acid-g-styrene), P(AA-g-S), graft copolymers by quantitative hydrolysis from poly(tert-butyl acrylate-g-styrene), P(tBA-g-S), precursors and evaluated by 1 H NMR and FTIR. The thermal characterization of these copolymers as a

function of the number of grafted repeat units was performed by differential scanning calorimetry (DSC), thermogravimetric analysis (TGA), and dynamic mechanical experiments (DMA). They observed a higher thermal stability of the PAA main chain by TGA as incompatible PS is grafted onto it. They also found that the presence of polar functional groups in the backbone chain leads to the formation of hydrogen bonds giving rise to a substantial modification of the linear viscoelastic response.

L. Melo et al studied the degradation reactions during sulphonation of poly(styrene-co-acrylic acid) used as membranes[6]. They synthesized a random copolymer of poly(styrene-co-acrylic acid) (PS-AA) in solution by radical polymerization and cross-linked with divinyl benzene partially. The copolymer (PS-AA) was sulphonated with different molar quantities (20-60%) of sulphuric acid (H_2SO_4) and acetyl sulphate (CH_3COOSO_3H). The characterization of sulphonated PS-AA materials was done by infrared spectroscopy (FTIR), differential scanning calorimetry (DSC), and molar mass by gel permeation chromatography (GPC). DSC thermograms (Figure 5) showed that sulphonation with H_2SO_4 decreases the glass transition values but CH_3COOSO_3H increases the glass transition, in comparison with the neat PS-AA.
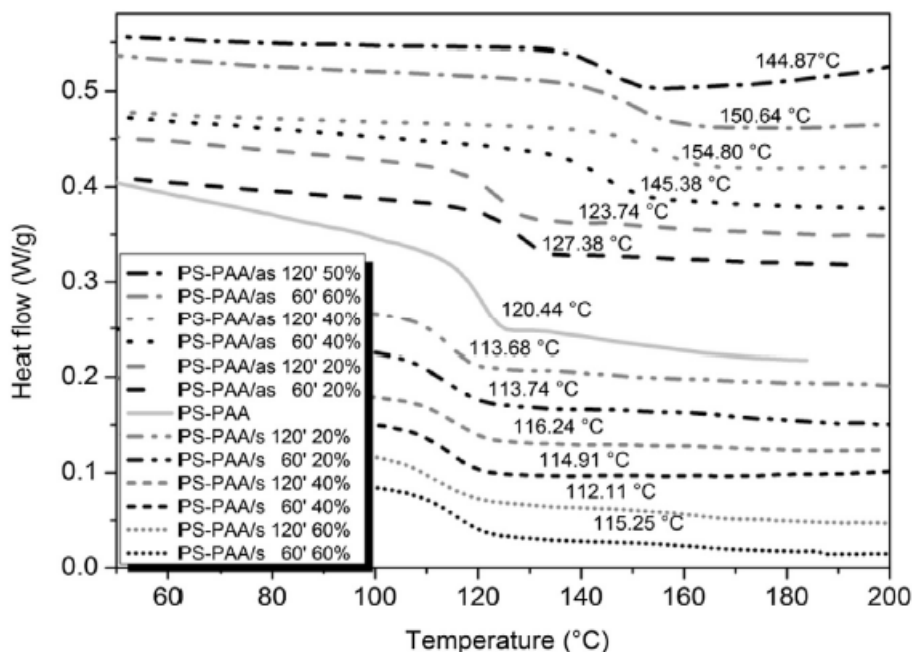
Figure 5: DSC thermograms of samples of PS-PAA

Clemente Bretti et al studied Interaction of acrylic-maleic copolymers with H^+, Na^+, Mg^{2+} and Ca^{2+} and their Thermodynamic parameters and their dependence on medium[7]. Potentiometric and calorimetric measurements were used to obtain thermodynamic parameters for the interaction of two acrylic-maleic copolymers with H^+, Na^+, Mg^{2+} and Ca^{2+}. Enthalpy changes for protonation, obtained by direct calorimetry were also expressed as a function of degree of dissociation (α) and I using empirical equations. The obtained formation constants for complexes of alkaline earth metal and alkali metals are quite low for Na^+ species. Depending on a and on ionic strength, they found $K < 10$ L mol^{-1} , and fairly high for Mg^{2+} and Ca^{2+} species, ML and ML_2 .

2.2 Terpolymers of Acrylic acid

The terpolymers of acrylic acids are not as common as their copolymers. As in the case of copolymers, styrene and maleic acid are most preferred comonomers for terpolymer of acrylic acid. Hatice Kaplan Can et al studied the Radical Terpolymerization of Maleic anhydride, Acrylic acid and Vinyl acetate and the effect of H-bonding[8]. They also substituted acrylic acid with methyl acrylate. The ternary copolymerization of vinyl acetate (VA), maleic anhydride (MA) and acrylic acid (AA) or methylacrylate (MAc as a model comonomer), considered as donor-acceptor-acceptor systems, was carried out in p-dioxane in the presence of benzoyl peroxide (BPO) as initiator in nitrogen atmosphere at 70°C. Differential scanning calorimetry (DSC)(Figure 6) and Thermogravimetric analysis (TGA) was carried out to compare the VA—MA—AA) and VA —MA—MAc terpolymers.
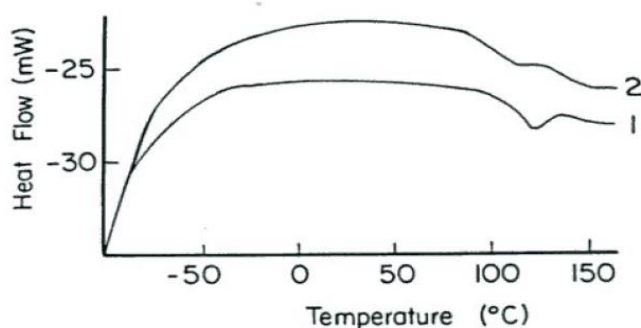
Figure 6: DSC curves of VA—MA—AA and VA—MA—MAc terpolymers recorded beginning from —100°C.

17

Poly(AA-co-MA-co-VA) terpolymers with different composition have characteristic glass-transition endotherms (Tg) in the field of 146.0, 153.5, 186.5 and 197.5°C. DSC curves of poly(AA-co-MA-co-VA) and poly(VA-co-MA-co-MAc) terpolymers recorded beginning -100°C showed that Tg endotherm is essentially shifted to relatively low temperature region (from 186.5 to 125°C for poly(AA-co-MA-co-VA) terpolymer). This fact can be explained by change of crystallization mechanism and by formation of more strong H-compelled macromolecules with different physical structural segments in lower temperature condition. Such crystalline phase is formed through intermolecular H-bonding between free -COOH group containing functional macromolecules.

Inderjeet Kaur and co-workers synthesized and characterized Acrylic acid Grafted Styrene-Maleic anhydride Copolymer[9]. They carried out the modification of Styrene-maleic anhydride copolymer, synthesized in toluene using benzoyl peroxide (BPO) as initiator, through graft copolymerization of hydrophilic monomer, acrylic acid, in aqueous medium by chemical and gamma radiation methods. Swelling studies of the grafted styrene-maleic anhydride copolymers, SMA-g-poly (AAc), was studied as a function of temperature, time and pH. Grafting % was studied as a function of amount of acrylic acid present (Figure 7).

Figure 7: Effect of amount of SMA on percent grafting of AAc

At higher amount of the monomer, homopolymer formation becomes the preferred process since the growing polymeric chains react with the monomer units lying close in the vicinity. The homopolymer, poly (AAc), thus formed, being soluble in water increases the viscosity of the

18

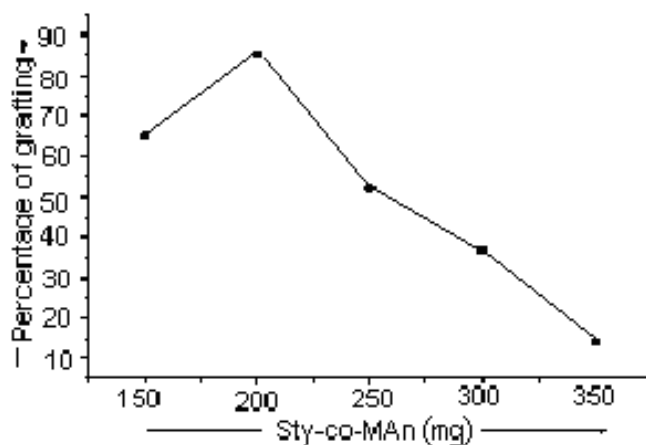medium their by restricting the mobility of the growing polymeric chains to the active sites leading to decrease in grafting %. Percentage of grafting increases with increasing time of reaction giving maximum (85%) in 180 minutes beyond which it decreases while with increasing temperature, maximum grafting (95%) was obtained at 70°C beyond which it decreases.

It was observed that Percentage of grafting (Pg) increases with increasing amount of BPO, giving maximum (85%) using 12.38×10^{-4} moles of BPO beyond which it decreases slightly. As the amount of BPO increases, generation of active sites on the SMA copolymer and initiation of monomer toward polymerization takes place that leads to increase in percent graft copolymer formation. It was also observed from the percentage of grafting increases when the amount of water was increased from 10 to 20 ml, where maximum grafting (85%) was observed. Percentage of grafting remains constant with further increase in the amount of water.

Pentablock terpolymers of acrylic acid are also present in literature. James G. Kopchick et al synthesized pentablock terpolymer of acrylic acid with styrene and isobutylene and carried out its morphological characterization[10]. The morphologies poly[acrylic acid-b-styrene-b-isobutylene-b-styrene-b-acrylic acid] pentablock terpolymers were investigated using transmission electron microscopy, atomic force microscopy, small angle X-ray scattering, and indirectly by dynamic mechanical analysis and degree of water sorption after synthesis. Transmission electron microscopy images (Figure 8) showed regions of polystyrene and Polyacrylic acid.
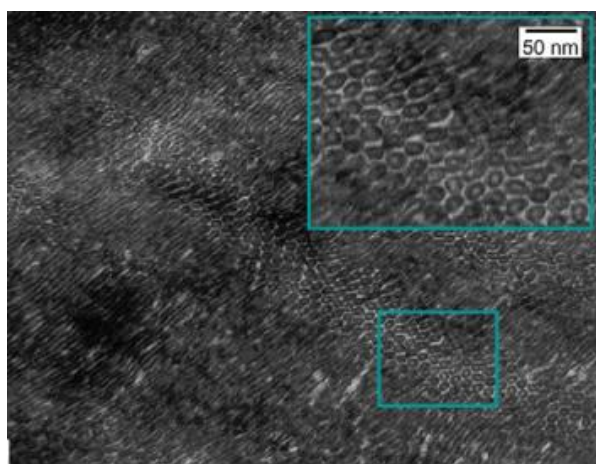

Figure 8: Transmission electron microscopy images pentablock terpolymer (23.4% PAA) sample stained with RuO4, then OsO4.

It was suggested that dark areas are Polystyrene cylinders while inner regions are of polyacrylic acid and the continuous phase is of Polyisobutylene composition. The three-phase morphology in this image appeared to be that of PAA cylinders within cylinders of PS. The white areas attributed to PAA are more continuous and are seen in nearly every cylinder which suggested more continuity or extension, of the PAA phase. To be sure, identifying this morphology as cylindrical at this point is speculation. On the basis of block sequence, it would seem that PAA domains should reside within the PS domains. Due to the similar PAA, PIB and PS percent compositions, samples B (23.4% PAA) and C (24.0% PAA) are expected to have similar morphologies. However, on the basis of simple visual and handling inspection, there were differences. Sample C had pits in surfaces and was less flexible than sample B. Also sample C (24.0% PAA) absorbs a larger amount of water as compared to sample because of the higher % of polyacrylic acid.

2.3 Composites and coatings of Polyacrylic acid

Composites of Polyacrylic acid with nanoparticles are quite common and there is large amount of literature present on this area of research. Polyacrylic acid coated nanoparticles are also a new developing area. Behnaz Hojjati et al synthesized TiO_2/PAA nanocomposite by RAFT polymerization[11]. There is a Strong tendency of nanoparticles such as metal oxides to agglomerate, therefore, homogeneous dispersion of these materials in a polymeric matrix is difficult. In order to overcome this problem and to enhance the filler-polymer interaction, they focused their study on living polymerization that was initialized from the surface of Titanium dioxide nanofillers.
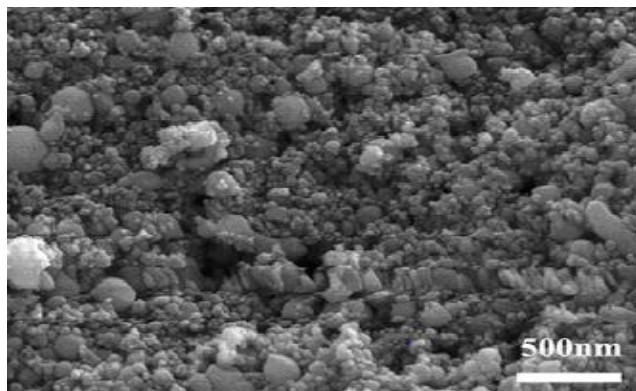

Figure 9: n-TiO_2/PAA nanocomposite

Figure 9 showed the n-TiO$_2$/PAA nanocomposite formed after grafting from polymerization with Acrylic acid in which many nanoparticles with a diameter 20-400 nm can be observed. These are attributed to the polymer chains that can only grow from the RAFT agent attached to the n-TiO$_2$ surface, resulting in the formation of n-TiO$_2$/PAA nanocomposite. The method for synthesizing TiO$_2$/polymer nanocomposites was found with a good dispersion of the nanofillers by using 2-{[(butylsulfanyl)carbonothioyl]sulfanyl}propanoic acid) , the bifunctional RAFT agent. This RAFT agent has an available carboxyl group to anchor onto TiO$_2$ nanoparticles, and an S=C(SC$_4$H$_9$) moiety for subsequent RAFT polymerization of acrylic acid (AA) to form n-TiO$_2$/PAA nanocomposites.

H.A. Ali and A.A. Iliadis prepared poly(styrene–acrylic acid) ZnO nanocomposite thin films on Silicon and silicon dioxide substrates[12]. The polystyrene–polyacrylic acid copolymer consisting of a majority block of polystyrene and a minority block of polyacrylic acid with a block number average molecular weight ratio of 16,500/4500 and a block repeat unit ratio of 159/63 was used in order to obtain self-assembly due to microphase separation with spherical morphology. Photolithographic techniques were used to apply the polymer films by standard spin-on on Silicon wafers with and without thermally grown SiO$_2$ surface films. The introduction of the ZnO nanoparticles followed by doping the copolymer with a ZnCl$_2$ precursor in liquid phase at room temperature, and then, upon solidification, by converting the precursor into ZnO using both a wet chemical process and a new dry ozone process. The new process resulted in effectively converting the ZnCl$_2$ precursor into ZnO in a significantly less time than the wet process.

Zhexiong Tang, Neil Alvarez and Sze Yang prepared CeO nanocomposites with polyaniline and polyacrylic acid for coating on aluminium and glass substrate[13]. The organic component of the hybrid material was an inter-polymer complex of conducting polymer. This molecular complex consisted of two polymers polyaniline and polyacrylic acid that form a double-strand molecular complex. The first strand was polyaniline (PAN), and the second strand was a polymeric dopant, e.g., poly(acrylic acid), (PAA). The two strands of the component polymers were non-covalently bonded in a largely side-by-side arrangement. Figure 10 shows that the visible absorption spectrum of the dispersion has electronic absorption bands identical to that of the PAN-PAA complex.
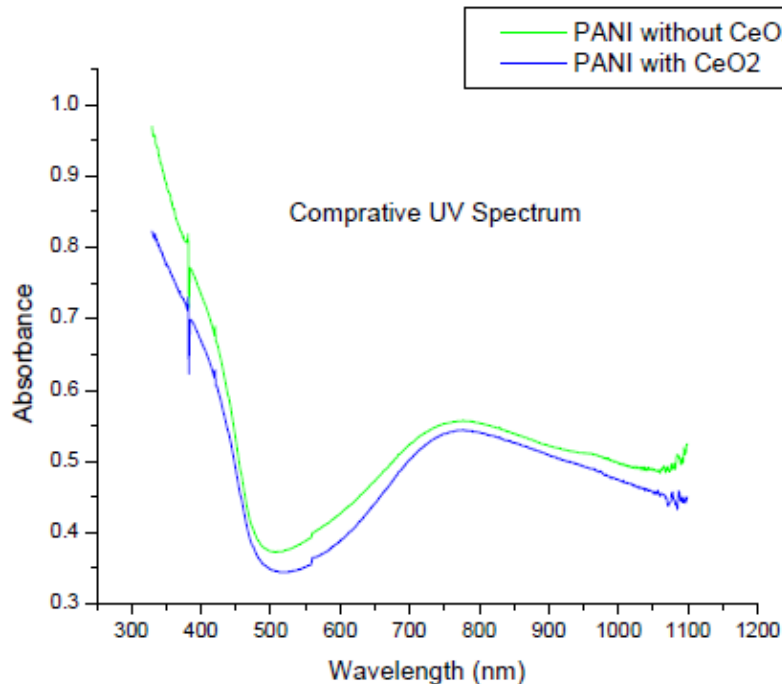
Figure 10: UV-Vis absorption spectra of the PAN-PAA complex (green curve) and the(PAN-PAA):CeO_2 composite.

The CeO_2 component of the composite does not show significant effect on the optical absorption spectrum in the visible spectral range. The presence of the polymeric ionic dopant (PAA) enables the polymeric complex to be dispersible in water. In contrast, the conventional small ion doped polyaniline is insoluble and is difficult to process.

Polyacrylic acid is also suitable for the biomedical applications. Its hydrophilicity makes it compatible with biological systems. E. De Giglio et al synthesized polyacrylic acid to deposit them on orthopedic implants. They deposited polyacrylic acid onto titanium based implants using electrodeposition method[14]. Their approach was to increase the biocompatibility of the metal based implants. The chemical structure of the PAA coating was investigated by X-ray photoelectron spectroscopy (XPS). Scanning electron microscopy (SEM) (figure 11) was employed to evaluate the effect of annealing treatment on the morphology of the coatings in terms of their uniformity and porosity.
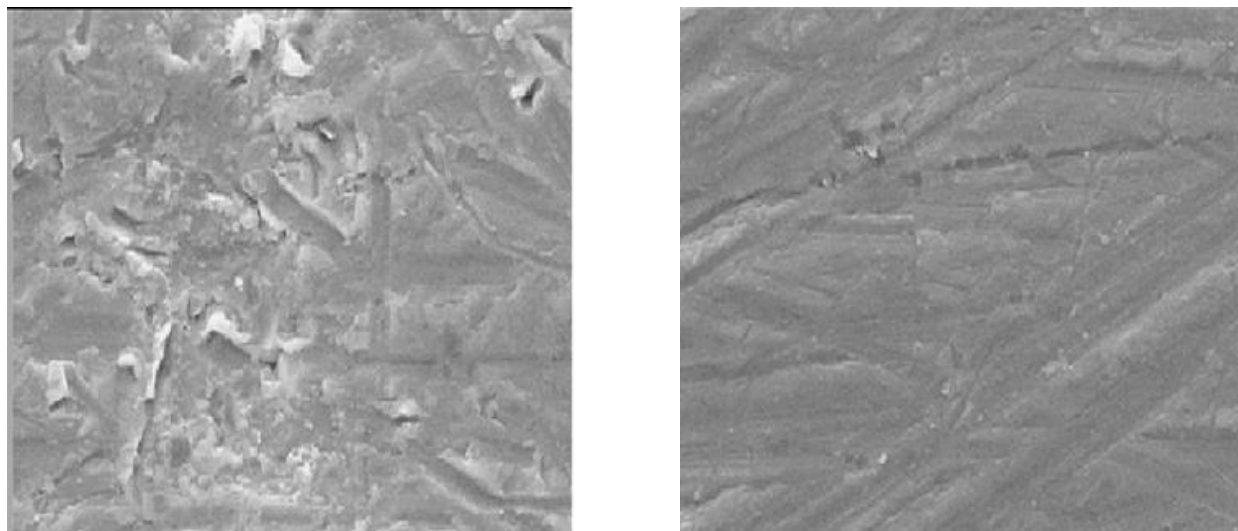
(a) (b)

Figure 11: SEM micrographs of PAA films that were electrochemically grown on titanium sheets at final CV potentials of −1.6 V, before (a) and after (b) annealing

Morphological examination was carried out by SEM in order to evaluate the effect of the annealing treatment. All PAA coatings were observed to be opaque; SEM examinations confirmed that this was due to a rough surface morphology with many small grainy deposits on the surface (Figure 11). As far as annealing is concerned, the annealed PAA coatings looked transparent and SEM analysis suggested that they became much smoother and more compact. Results indicated that the annealing process produces coatings that possess considerable anti-corrosion performance. Moreover, the availability and the reactivity of the surface carboxylic groups were exploited in order to graft biological molecules onto the PAA-modified titanium implants. The final result of their study is the development of modified PAA films that combine the potential to graft on biologically active molecules in order to improve biological performance with the ability to provide protection against the corrosion of titanium-based implants, which is a pressing need in orthopaedic field implant applications.

There are examples available in which polyacrylic acid is used to modify the surface of nanoparticles. Some other inorganic substances like silica or alumina can also be used for the same purpose. Surface modification of rutile TiO_2 nanoparticles with SiO_2/Al_2O_3 and its composite with polyacrylic acid was developed by J. Godnjavec et al[15]. For the improvement of

nanoparticles dispersion and the decreasing of photocatalytic activity, the surface of nanoparticles was modified with binary SiO_2/Al_2O_3. The surface treatment of TiO_2 nanoparticles was characterized with FTIR (Figure 12). Microstructural analysis was done by AFM. The size, particle size distribution and zeta potential of TiO_2 nanoparticles in water dispersion was measured by DLS technique.
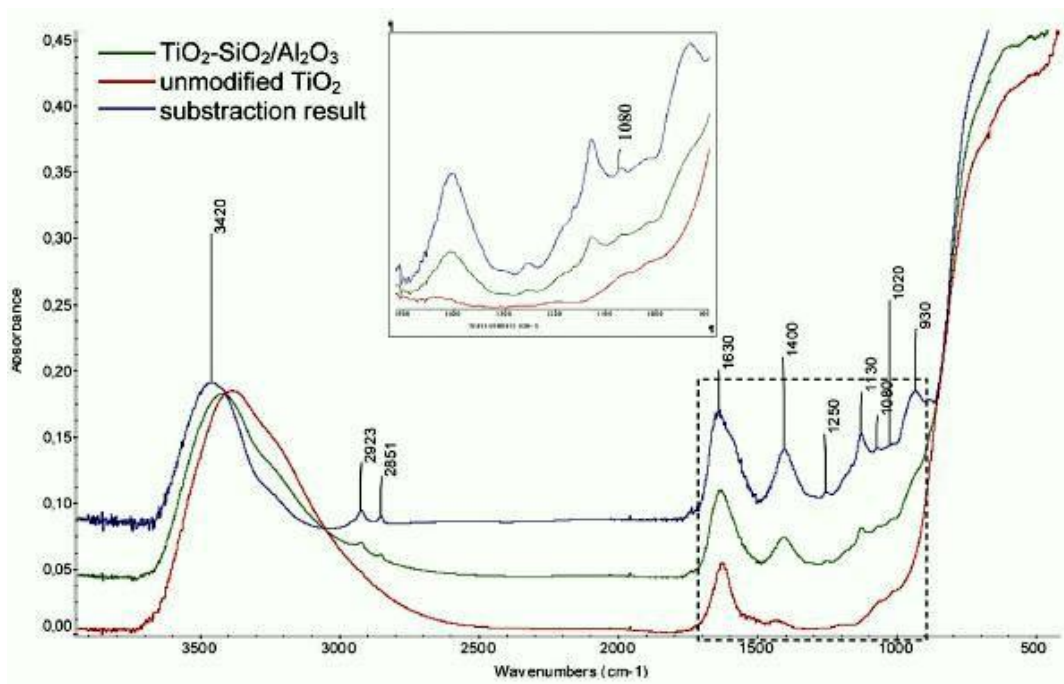
Figure 12: FTIR spectra of unmodified TiO_2, TiO_2–SiO_2/Al_2O_3 nanoparticles and substraction result.

In the FTIR spectra, OH groups are described by bands at 3420 and 1630 cm^{-1}. The band appearing at 930 cm^{-1} is due to Si-O-Ti stretching vibration. The Al_2O_3 layers were probably anchored at the SiO_2 coated TiO_2 via Al-O-Si bond around 1080 cm^{-1}. Al-O stretching vibration is present at 1020 and 1130 cm^{-1} in the spectra. Also, the small peak around 600 cm^{-1} originates due to Al-O stretching vibration. Peak at 1400 cm^{-1} is assigned to TiO_2–SiO_2 groups. There are also some bands in the spectra at 2923, 2851 and 1250 cm^{-1} that are assigned to organic

24

modification residue. The results of FTIR analysis showed that in the case of sample TiO_2–SiO_2/Al_2O_3, TiO_2 nanoparticles were successfully modified with SiO_2 and with Al_2O_3.

Iron oxide nanoparticles can also be modified by polyacrylic acid. Y. Xu et al modified the amino acid functionalized magnetite Fe_3O_4 nanoparticles with the help of polyacrylic acid[16]. Fe_3O_4 nanoparticles modified with polyacrylic acid (PAA) were prepared using a solvothermal approach. The adsorption behavior of Glycine, L-Arginine and L-Tyrosine on the PAA coated Fe_3O_4 nanoparticles was investigated, and the adsorption isotherm of these amino acids on magnetite nanoparticles at different pH values was described. The amount of amino acid adsorbed increases as the concentration of amino acid is increased.
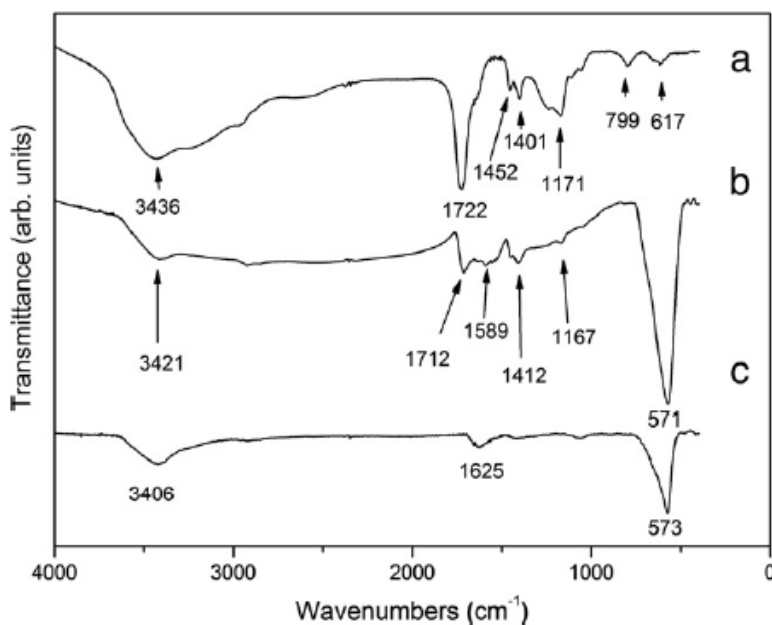
Figure 13: FTIR spectra of (a) PAA, (b) PAA modified magnetic particles, and (c) bare magnetic particles.

The samples were characterized by FTIR spectroscopy. FTIR spectra (Figure 13) there is no C=C stretching vibration absorption peak around 1600 cm^{-1}, which indicates that no AA monomer remains in PAA. The peaks at 570 cm^{-1} in Figure 13 b and c confirm that the product is Fe_3O_4. The C=O stretching vibration peak (1712 cm−1), C-O-C stretching vibration peak

25

(1167 cm^{-1}) and the characteristic absorption peaks of carboxylate at 1589 cm^{-1} and 1412 cm^{-1} in Figure b confirmed the chemisorption of PAA on the surface of the Fe_3O_4 particles. By comparing these spectra, it was clear that a large number of carboxylate groups remained on the surface of the nanoparticles. This result also indicated that part of the uncoordinated carboxylate groups on the polymer chains extended into the aqueous solution, conferring upon the particles a high degree of dispersibility in water.

One of the biomedical applications of polyacrylic acid is bone fillers. Synthesis and characterization of Brittle and ductile adjustable cement derived from calcium phosphate cement (CPC)/polyacrylic acid composites was done by Wen-Cheng Chen et al[17]. they characterized a non-dispersive, fast setting, modulus adjustable, high bioresorbable composite bone cement derived from calcium phosphate-based cement combined with polyacrylic acid and binding agents. When the polyacrylic acid/CPC weight ratio increased to 67 and 100 weightt %, the specimens kept at saturated humidity for 24 h revealed ductile–soft properties.

The results showed that while composite, the hard–brittle properties of 25 wt% polyacrylic acid are proportional to CPC and mixing with additives is the same as those of the CPC without polyacrylic acid added. With an increase of polyacrylic acid/CPC ratio, the 67 wt% samples revealed ductile–tough properties and 100 wt% samples kept ductile or elastic properties after 24 h of immersion.

CHAPTER 3   **EXPERIMENTAL**
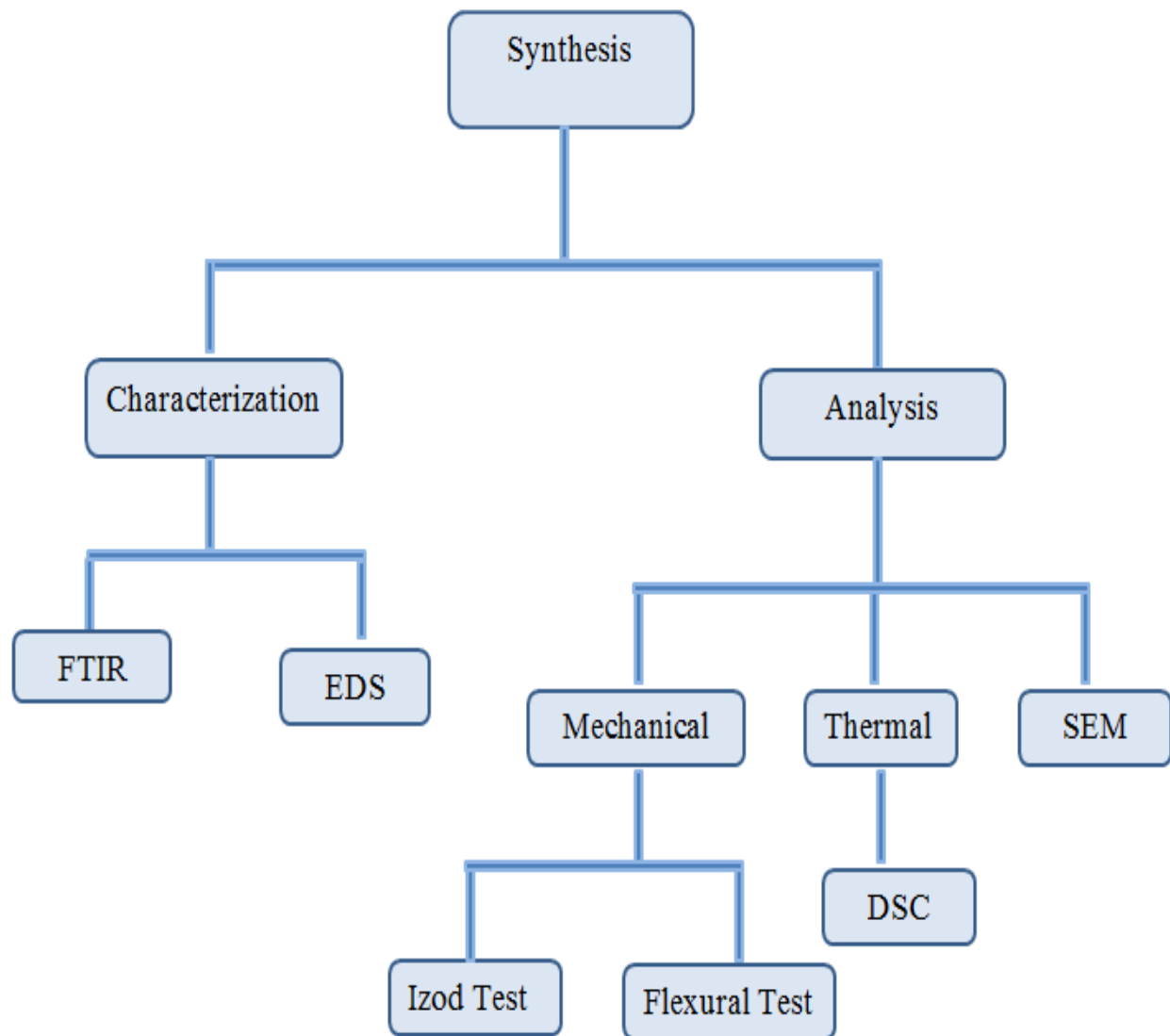
Work Plan

3.1 Chemicals/Materials

Styrene was purchased from Alpha Ceaser, Great Britain. Titanium dioxide and Alumina was purchased from Molychem, India. Benzoyl peroxide, sodium hydroxide, acrylic acid, and maleic anhydride were obtained from Central Drug House, Delhi. The glass used was Soda-lime glass.

3.2 Synthesis

The acrylic acid-styrene-maleic anhydride terpolymers of different compositions were synthesized using bulk polymerization [Scheme 1]. Acrylic acid and styrene usually contain some inhibitors. 30 ml of both acrylic acid and styrene were taken in a separatory funnel and washed with 10% NaOH solution several times to remove the inhibitors completely. Then acrylic acid and styrene were washed with water several times to remove the NaOH and dried using anhydrous $CaCO_3$.
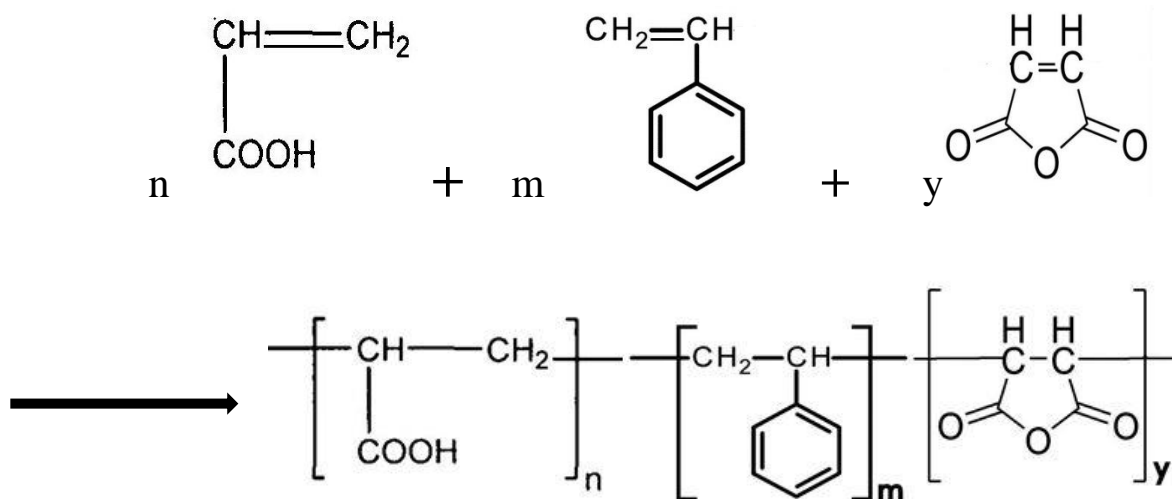
Scheme 1: synthesis of Acrylic acid-styrene-maleic anhydride terpolymer

To synthesize the polyacrylic acid (PAA) as reference polymer, 20 g (21ml) purified acrylic acid was taken in a beaker and heated with 50 mg benzoyl peroxide at temperature of 70°C for 20 minutes. To synthesize the acrylic acid-styrene-maleic anhydride terpolymer, acrylic acid was mixed with styrene and then maleic anhydride was dissolved in above solution. The prepared solution was polymerized using benzoyl peroxide and the same conditions of temperature and time used for the synthesis of PAA.

3.3 Preparation of Composite

The terpolymer **ASM73** and **ASM74** showed much higher mechanical strength than other samples and therefore selected for the preparation of composites. They were dissolved in minimum amount of 10 % NaOH Solution to obtain a viscous solution. Composites were

prepared by the addition of the respective amounts of TiO_2 and Al_2O_3 to the solution of terpolymers in NaOH with constant stirring for proper mixing. It has been found that the preparation of **ASM73 C** with 0.5 % TiO_2 and 0.25 % Al_2O_3 (by weight) resulted in loss of its clarity. So the composite **ASM74 C** was prepared with 0.25 % of both TiO_2 and Al_2O_3 (by weight) and it showed good clarity. The compositions of terpolymers and the amounts of constituents are shown in table 1.

Table 1: Polymers and their compositions showing percentage (by Wt) of constituent

S.No	Polymer	Percentage (by Wt) & Amount				
		Acrylic acid	Styrene	Maleic anhydride	TiO_2	Al_2O_3
1	PAA	100 % (20 g)	-	-	-	-
2	ASM52	93 % (18.6 g)	5 % (1 g)	2 % (0.4 g)	-	-
3	ASM73	90 % (18 g)	7 % (1.4 g)	3 % (0.6 g)	-	-
4	ASM74	89 % (17.8 g)	7 % (1.4 g)	4 % (0.8 g)	-	-
5	ASM73 C	89.25 % (17.8 g)	7 % (1.4 g)	3 % (0.6 g)	0.5 % (0.1 g)	0.25 % (0.05 g)
6	ASM74 C	88.50 % (17.7 g)	7 % (1.4 g)	4 % (0.8 g)	0.25 % (0.05 g)	0.25 % (0.05 g)
7	ASM102	88 % (17.6 g)	10 % (2 g)	2 % (0.4 g)	-	-
8	ASM103	87 % (17.4 g)	10 % (2 g)	3 % (0.6 g)	-	-
9	ASM104	86 % (17.2 g)	10 % (2 g)	4 % (0.8 g)	-	-

3.4 Coating on glass substrate

The **PAA** and the terpolymer synthesized were dissolved in 10 % NaOH so that it can be applied on the substrate easily. NaOH being a base reacts with the acidic group –COOH to form salt (-COONa). This salt of polyacrylic acid and the terpolymer has better adhesion strength as compared to polyacrylic acid and terpolymer containing –COOH group. The solutions of polyacrylic acid, terpolymers and the composites were applied to the glass slide and spread evenly with the help of a glass rod to obtain a smooth surface with constant thickness. After the coating, the samples were cured at 100°C in oven for 24 hrs to obtain a clear hard coating on glass.

3.5 Characterization

3.5.1 Fourier transform infrared (FTIR) Analysis

Infrared (IR) spectroscopy is one of the most common spectroscopic techniques used by organic and inorganic chemists. Simply, it is the absorption measurement of different IR frequencies by a sample positioned in the path of an IR beam. The main goal of IR spectroscopic analysis is to determine the chemical functional groups in the sample. Infrared spectroscopy has been a workhorse technique for materials analysis in the laboratory for over seventy years. An infrared spectrum represents a fingerprint of a sample with absorption peaks which correspond to the frequencies of vibrations between the bonds of the atoms making up the material. Because each different material is a unique combination of atoms, no two compounds produce the exact same infrared spectrum. Therefore, infrared spectroscopy can result in a positive identification (qualitative analysis) of every different kind of material. In addition, the size of the peaks in the spectrum is a direct indication of the amount of material present.

Different functional groups absorb characteristic frequencies of IR radiation. Using various sampling accessories, IR spectrometers can accept a wide range of sample types such as gases, liquids, and solids. In this experiment Fourier transform infrared (FTIR) spectroscopy was used to determine the important groups such as carboxylic acid –COOH, carbonyl group C=O and phenyl ring. To carry out the FTIR, sample powder is mixed with KBr to prepare a 10% by

weight mixture. This mixture was used to prepare pellets of 1 cm diameter. These pellets were placed in sample holder and then exposed to infrared rays to obtain the graph.

Figure 14: Thermo Scientific Nicolet 380 Spectrometer

Apparatus Specifications

Apparatus: Thermo Scientific Nicolet 380 Spectrometer (Figure 14)

Spectral range - 7800 – 350 cm^{-1} using proprietary KBr beam splitter.

Optical resolution < 0.9 cm^{-1} resolution (standard)

Wavenumber precision- Better than 0.01 cm^{-1} precision at 2000 cm^{-1}

3.5.2 Energy-dispersive X-ray spectroscopy(EDS)

EDS[18] makes use of the X-ray spectrum emitted by a solid sample bombarded with a focused beam of electrons to obtain a localized chemical analysis. All elements from atomic number 4 (Be) to 92 (U) can be detected in principle, though not all instruments are equipped for 'light' elements (Z < 10). Qualitative analysis involves the identification of the lines in the spectrum and is fairly straightforward owing to the simplicity of X-ray spectra. Quantitative analysis (determination of the concentrations of the elements present) entails measuring line   intensities

31

for each element in the sample and for the same elements in calibration Standards of known composition.

By scanning the beam in a television-like raster and displaying the intensity of a selected X-ray line, element distribution images or 'maps' can be produced. Also, images produced by electrons collected from the sample reveal surface topography or mean atomic number, according to the mode selected. The scanning electron microscope (SEM), which is closely related to the electron probe, is designed primarily for producing electron images, but it can also be used for element mapping, and even point analysis, if an X-ray spectrometer is added. EDS was done by Hitachi Hi Technologies Scanning Electron Microscope S-3700 N.

3.6 Analysis Techniques

3.6.1 Scanning Electron Microscopy (SEM)

SEM was carried out to study the morphology of the polymers produced. A scanning electron microscope (SEM) is a type of electron microscope that produces images of a sample by scanning it with a focused beam of electrons. The electrons interact with electrons in the sample, producing various signals that can be detected and that contain information about the sample's surface topography and composition. The electron beam is generally scanned in a raster scan pattern, and the beam's position is combined with the detected signal to produce an image. SEM can achieve resolution better than 1 nanometer. Specimens can be observed in high vacuum, in low vacuum, and (in environmental SEM) in wet conditions.

The most common mode of detection is by secondary electrons emitted by atoms excited by the electron beam. The number of secondary electrons is a function of the angle between the surface and the beam. On a flat surface, the plume of secondary electrons is mostly contained by the sample, but on a tilted surface, the plume is partially exposed and more electrons are emitted. By scanning the sample and detecting the secondary electrons, an image displaying the tilt of the surface is created. SEM was done by Hitachi Hi Technologies Scanning Electron Microscope S-3700 N.

Apparatus specification-

Apparatus used-Hitachi Hi Technologies Scanning Electron Microscope S-3700 N (Figure 15)

Specimen size - 1x1 cm

Operating voltage - 2.5kv 15 kv

Resolution- 3.0 nm at 30 kV (High vacuum mode)

Magnification- ×5 - ×300,000

Figure 15: Hitachi Hi Technologies Scanning Electron Microscope S-3700N

3.6.2 Thermal Analysis

3.6.2.1 Differential Scanning Calorimetry (DSC)

A differential scanning calorimeter measures the heat of sample relative to a reference and heats the sample with a linear temperature ramp. Endothermic heat flows into the sample. Exothermic heat flows out of the sample. Differential Scanning Calorimetry (DSC), measures the heat flows and temperatures associated with transitions in materials as a function of time and temperature in a controlled atmosphere. These measurements provide quantitative and qualitative information about physical and chemical changes that involve endothermic or exothermic processes or changes in heat capacity.

Differential scanning calorimetry (DSC) monitors heat effects associated with phase transitions and chemical reactions as a function of temperature. In a DSC the difference in heat flow to the sample and a reference at the same temperature, is recorded as a function of temperature. The reference is an inert material such as alumina, or just an empty aluminum pan. The temperature of both the sample and reference are increased at a constant rate.

Apparatus Specifications

Apparatus - TA Instruments DSC Q20 (figure- 16)

Temperature Range   -Ambient to 725 ˚C

Temperature Accuracy   - +/- 0.1 ˚C

Sensitivity   -1.0 Mw

Fig 16: TA Instruments DSC Q20

3.6.3 Mechanical Testing

3.6.3.1 Flexural strength test

The behaviour of polymer to stress and strain in flexure is important for polymer manufacturer and designers. Flexural strength is the ability of the material to withstand bending forces applied perpendicular to its longitudinal axis. The stresses which flexural load generates are a

combination of tensile and compressive stresses. There are polymers that do not break when flexural loads are applied even after a large amount of deflection. Calculation of ultimate flexural strength of these polymers are difficult. But for those polymers which easily break under flexural stresses, the deflection is carried out till rupture occurs in the outer fibers.

Flexural strength can be determined by using two basic methods. These two methods are three point bending system and four point bending system. in the three point bending system, the specimen rests on two supports and load is applied by the loading nose midway between the supports. This system is generally used for those materials which easily break under flexural stress. In the present investigation, three point bending system is used to determine the flexural strength of coated glass The instrument used for this purpose was Instron Universal testing machine (UTM) 3369. The dimensions of the samples were 74 x 23.5 x 1.2 mm.

Figure 17: Instron Universal Testing machine 3369

Apparatus Specifications

Apparatus: Instron Universal Testing machine 3369[Figure 17]

Dual Column testing system

Capacity: 50 kN (11,250 lbf)

Maximum speed: 500 mm/min (20 in/min)

Vertical test space: 1193 mm (47 in)

3.6.3.2 Izod impact test

Impact tests are used in studying the toughness of material. A material's toughness is a factor of its ability to absorb energy during plastic deformation. Impact energy is a measure of the work done to fracture a test specimen. In this test a striker of known weight impacts the specimen, the specimen will absorb energy until it yields. At this point, the specimen will begin to undergo plastic deformation at the notch. The test specimen continues to absorb energy and work hardens at the plastic zone at the notch. When the specimen can absorb no more energy, fracture occurs. Brittle materials have low toughness as a result of the small amount of plastic deformation that they can endure. The impact value of a material can also change with temperature. Generally, at lower temperatures, the impact energy of a material is decreased. The size of the specimen may also affect the value of the Izod impact test because it may allow a different number of imperfections in the material, which can act as stress risers and lower the impact energy. The results are expressed in energy lost per unit of thickness (such as ft-lb/in or J/cm) at the notch. Alternatively, the results may be reported as energy lost per unit cross-sectional area at the notch (J/m² or ft-lb/in²). In Europe, ISO 180 methods are used and results are based only on the cross-sectional area at the notch (J/m²).The dimensions of the Izod specimens used were 74 x 12.7 x 1.2 mm

Apparatus Specification:

Apparatus: International equipment Izod/Charpy impact tester [Figure 18]

Capacity: Up to 21.68 Joules.

Release angle of pendulum: 150 degree.

Range of four scales: 0-2.71 Joules, 0-5.42 Joules,

0.1 Joule and 0.2 Joule respectively.

Power: 230 Volts, 50Hz, single phase.

Direct display through microcontroller: Impact energy in joules.

Figure 18: International equipment Izod/charpy impact tester

CHAPTER 4   **RESULTS AND DISCUSSION**

The poly(acrylic acid-styrene-maleic anhydride) terpolymers and its composites were prepared. These were characterized by Fourier transform infrared (FTIR) spectroscopy and Energy-dispersive X-ray spectroscopy (EDS). The mechanical properties of the terpolymers and composites were evaluated using Izod impact test and flexural strength test. DSC and Scanning electron microscopy was also performed.

4.1 Characterization

4.1.1 FTIR

Fourier transform infrared (FTIR) spectroscopy confirmed the presence of carboxylic group (-COOH), anhydride (CO-O-CO) group and phenyl ring in the poly(acrylic acid-styrene-maleic anhydride) terpolymer. In the FTIR spectrum of **PAA** (Figure19), the peak at 2936.5 cm^{-1} is due to –C-H symmetric and asymmetric stretch. The broad peak at 3469.9 cm^{-1} is due to O-H stretch and the peak at 1712.3 cm^{-1} is due to C=O group. Both these peaks confirmed the presence of –COOH group.
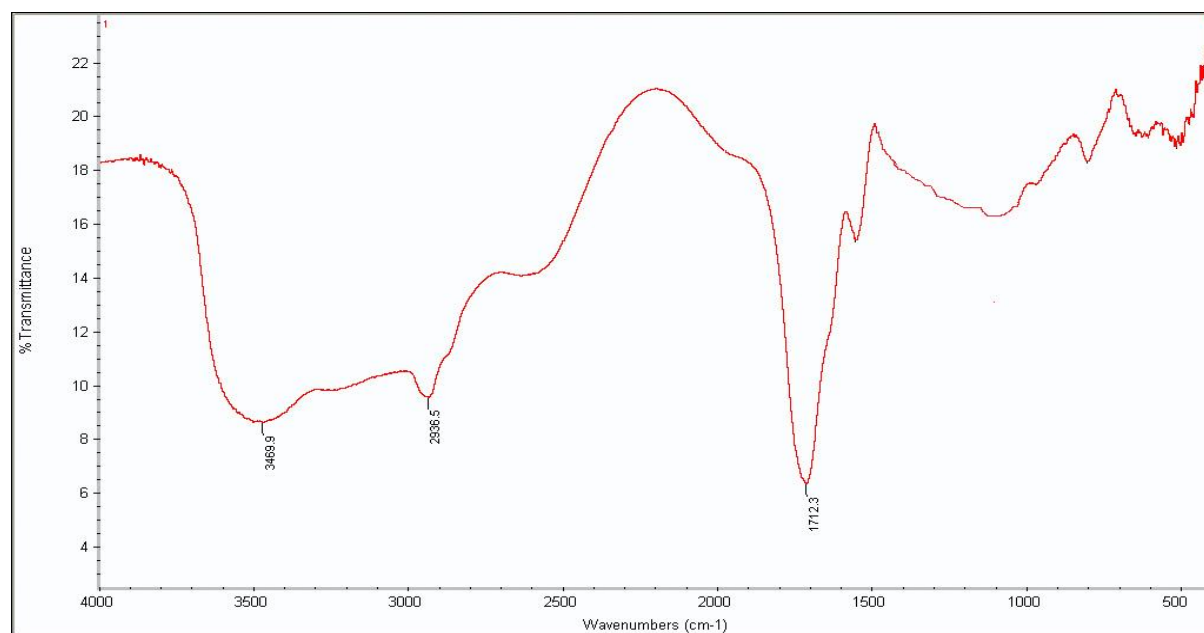

Figure 19: FTIR spectrum of **PAA**

The FTIR spectra of terpolymer **ASM73** and **ASM74** confirmed the presence of carboxylic group (-COOH), phenyl ring and anhydride (CO-O-CO) group in these two terpolymer. The broad peak at 3439.6 cm^{-1} in the FTIR spectrum of **ASM73** (Figure20) terpolymer shows the presence of –OH group. The peak at 1720.3 cm^{-1} is due to C=O group of –COOH. The peak at 1570.1 cm^{-1} is due to aromatic C-C=C group stretch. The peak at 625.6 cm^{-1} is due aromatic C-H bending which is the characteristic of aromatic group. The peak at 1039.9 cm^{-1} is due to the CO-O-CO stretch of the anhydride. So all these peak confirmed the presence of acrylic acid, styrene and maleic anhydride in the terpolymer.
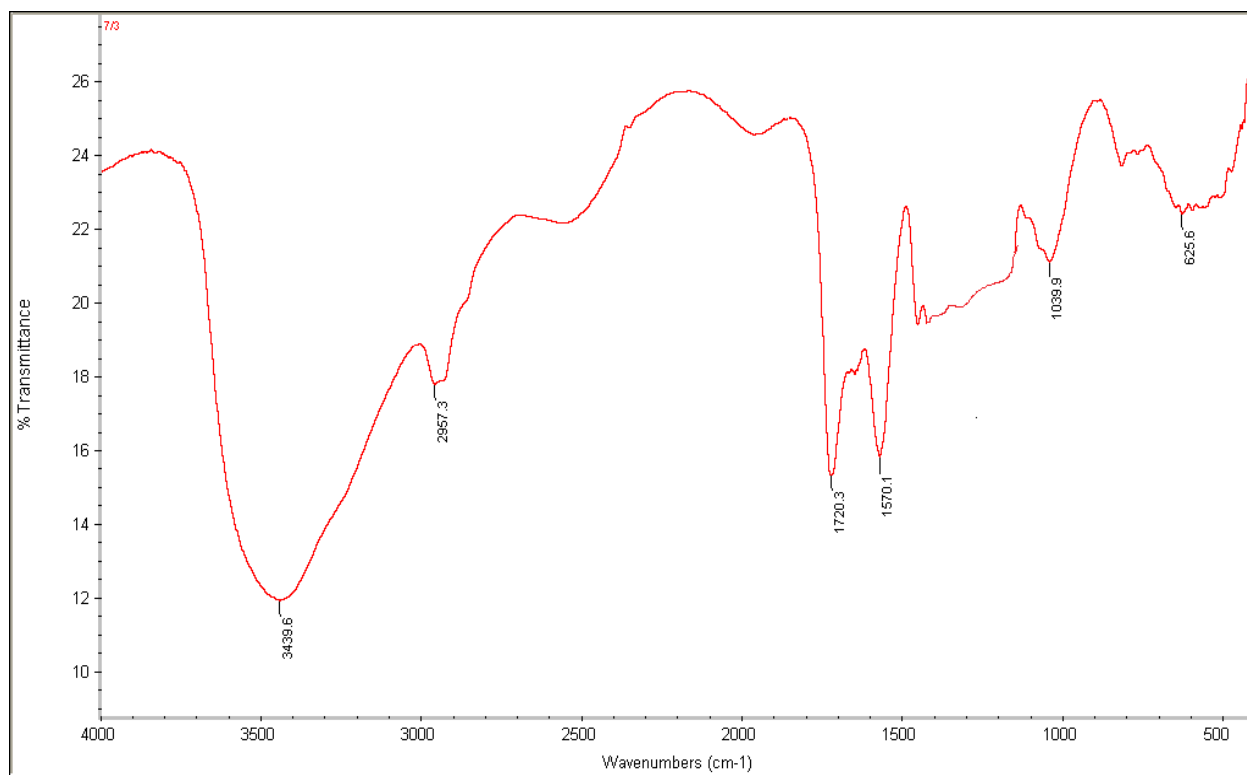

Figure 20: FTIR spectrum of **ASM73** terpolymer sample

The FTIR spectrum of the **ASM74** is similar to that of **ASM73** because both have same chemical constituents. In the FTIR spectra of **ASM74** (Figure 21) terpolymer, the broad peak at 3447.2 cm^{-1} shows the presence of –OH group and the peak at 1721.8 cm^{-1} is due to C=O group of –COOH. The peak at 1561.9 cm^{-1} is due to aromatic C-C=C group stretch. The peak at 821.7 cm^{-1} is due aromatic C-H bending which is the characteristic of aromatic group. The peak at 1030.7 cm^{-1} is due to the CO-O-CO stretch of the anhydride.
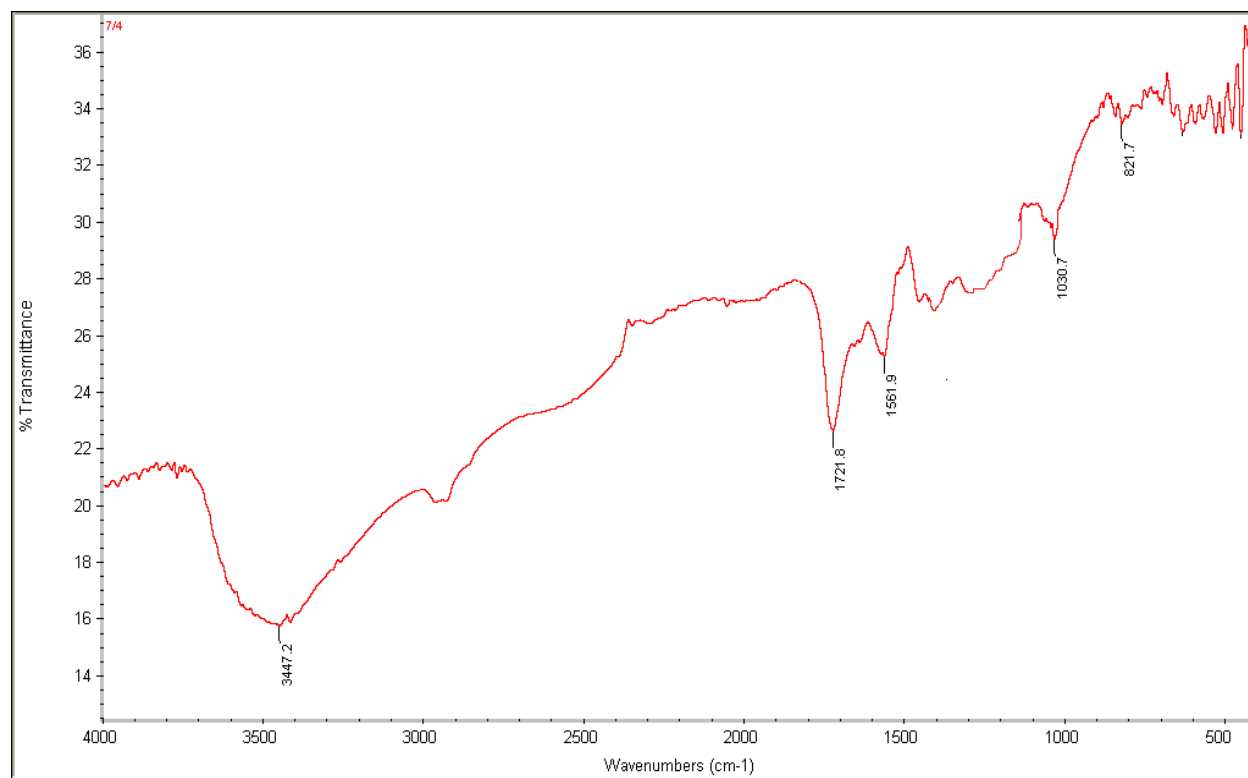
Figure 21: FTIR spectrum of **ASM74** terpolymer sample

The composite **ASM73 C** has same peaks in the region 3400- 3500, 1700-1600, 1100-1000 and 800-700 cm^{-1} due to OH, C=O, CO-O-CO and phenyl group respectively as that of **ASM73**. In the FTIR spectrum of **ASM73 C** composite (Figure 22), the peak in region 500-525 cm^{-1} is due Ti-O stretching. The peak in region 1280-1170 cm^{-1} is due to Al-O stretch. The peak in the region 1400-1410 cm^{-1} may be assigned to Ti-O-C bond [19], [20], [21] as is also reported in the literature. The spectrum of composite **ASM74 C** (Figure 23) is similar to that of terpolymer **ASM74** and it also possesses peaks in region the peaks at 1400-1410 cm^{-1} which may be assigned to Ti-O-C bond[19], [20], [21]. The peak in the region 1280-1170 cm^{-1} is due to Al-O bond respectively and the peak in region 500-525 cm^{-1} is due to the Ti-O stretching. So it can be deduced from the presence of peaks which probably shows the presence of Ti-O-C bond that there may be interaction between the inorganic and the organic moiety.
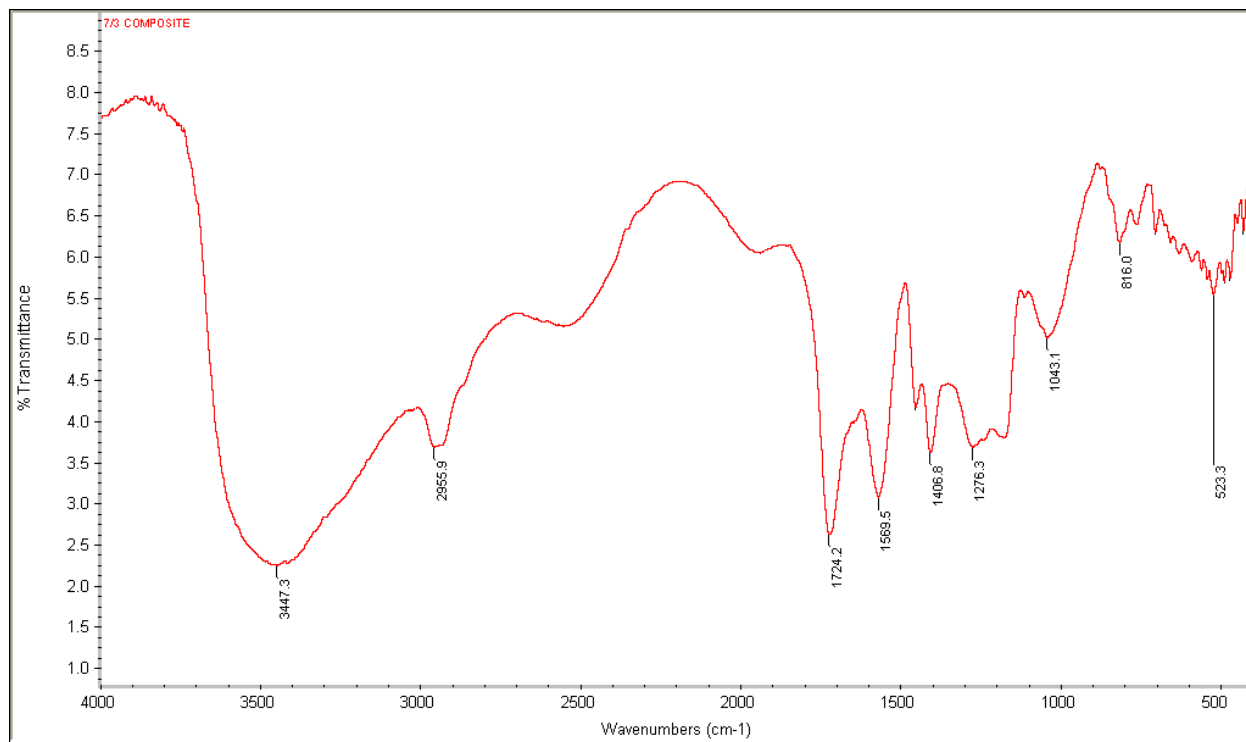
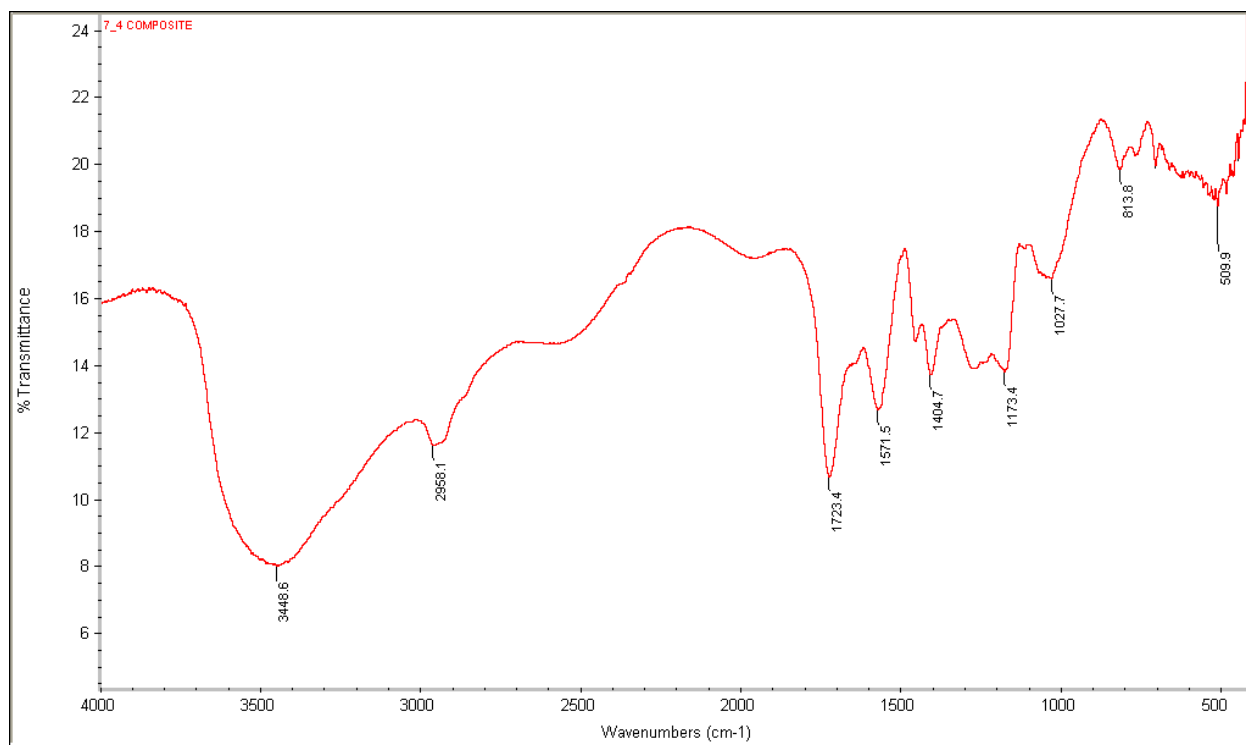Figure 22: FTIR spectrum of **ASM73 C** terpolymer sample

Figure 23: FTIR spectrum of **ASM74 C** terpolymer sample

4.1.2 Energy-dispersive X-ray spectroscopy (EDS)

Energy-dispersive X-ray spectroscopy (EDS) was used for elemental analysis of the terpolymers and the composite. In the present investigation, Energy-dispersive X-ray spectroscopy (EDS) is used to confirm the presence of TiO_2 and Al_2O_3 in the terpolymer composite and support the results of FTIR. The following figure 24 and table 2 shows the EDS spectrum of **ASM73 C** composite terpolymer and percentage of elements present in the terpolymer composite.
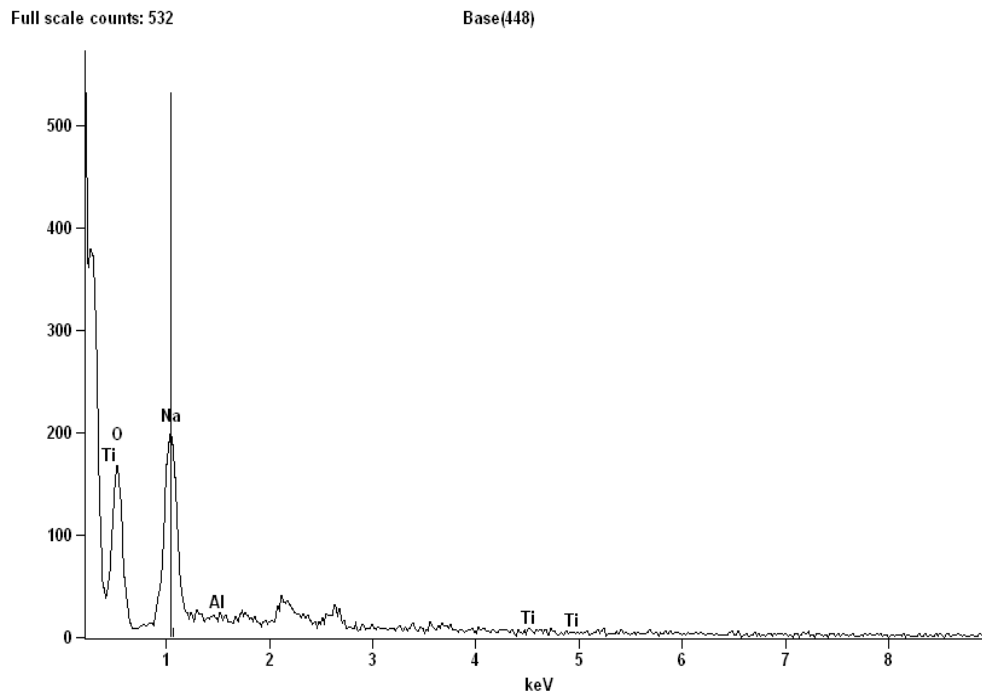

Fig 24: EDS spectrum of **ASM73 C** composite terpolymer

Table 2: Weight Percentage of elements present in **ASM73 C**

Element Line	Net Counts	Int. Cps/nA	Weight %	Weight % Error	Atom %	Atom % Error	Formula	Standard Name
O K	1504	---	45.85	+/- 1.28	55.39	+/- 1.55	O	
Na K	2271	---	51.13	+/- 1.62	42.99	+/- 1.36	Na	
Al K	50	---	1.26	+/- 0.58	0.90	+/- 0.42	Al	
Ti K	29	---	1.76	+/- 1.03	0.71	+/- 0.42	Ti	
Ti L	3	---	---	---	---	---		
Total			100.00		100.00			

Similarly, the figure 25 shows the EDS spectra of the terpolymer composite **ASM74 C**. The EDS results are tabulated in table 3 which shows the percentage of elements present in **ASM74 C**.
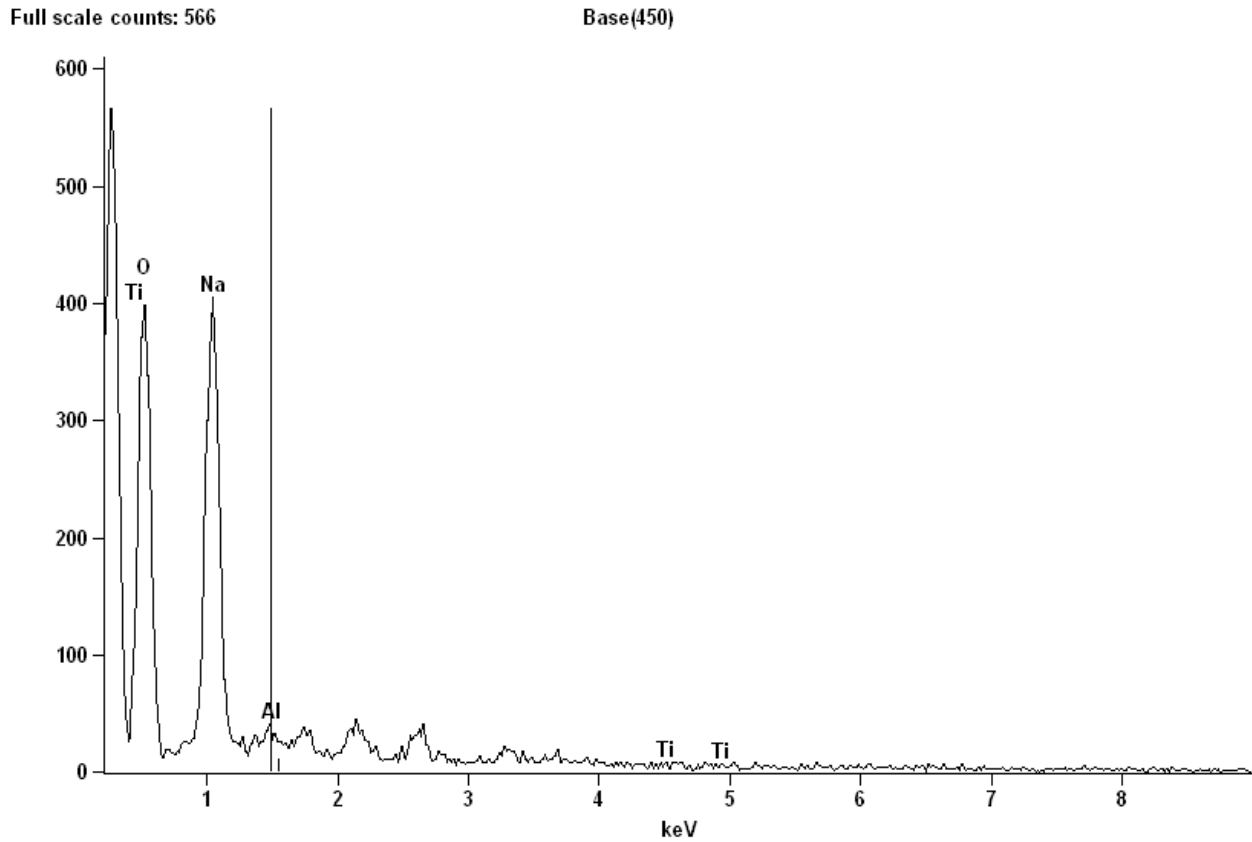
Full scale counts: 566   Base(450)

Fig 25: EDS spectra of the terpolymer composite **ASM74 C**

Table 3: Weight Percentage of Elements present in **ASM74 C**

Element Line	Net Counts	Int. Cps/nA	Weight %	Weight % Error	Atom %	Atom % Error	Formula	Standard Name
O K	3756	---	52.75	+/- 1.01	61.83	+/- 1.19	O	
Na K	3952	---	45.37	+/- 0.83	37.01	+/- 0.67	Na	
Al K	113	---	1.39	+/- 0.28	0.97	+/- 0.20	Al	
Ti K	16	---	0.49	+/- 0.43	0.19	+/- 0.17	Ti	
Ti L	0	---	---	---	---	---		
Total			100.00		100.00			

4.2 Analysis

4.2.1 Scanning electron microscopy (SEM)

Scanning electron microscopy was performed to study the morphology of the coatings. The surface of **PAA** and the terpolymer coatings were uniform and even. The composite coatings were uniform and even but not as uniform as terpolymer coatings. The SEM images are shown from figure 26 to 30.
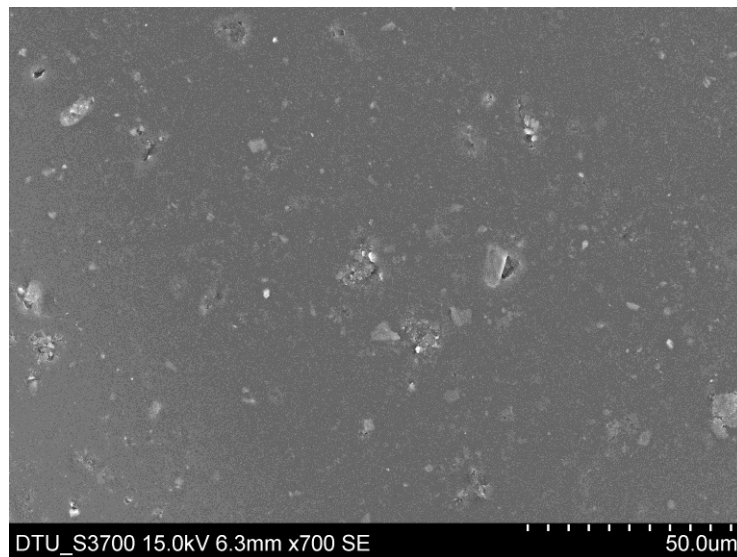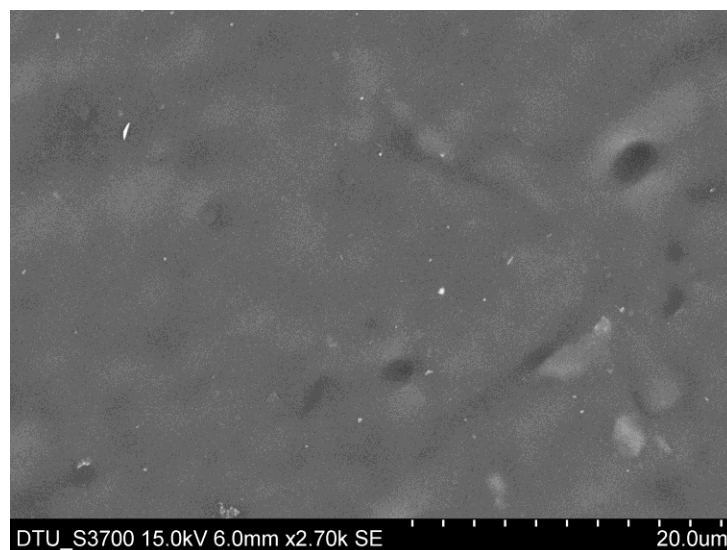
Fig 26: SEM image of **PAA** coating

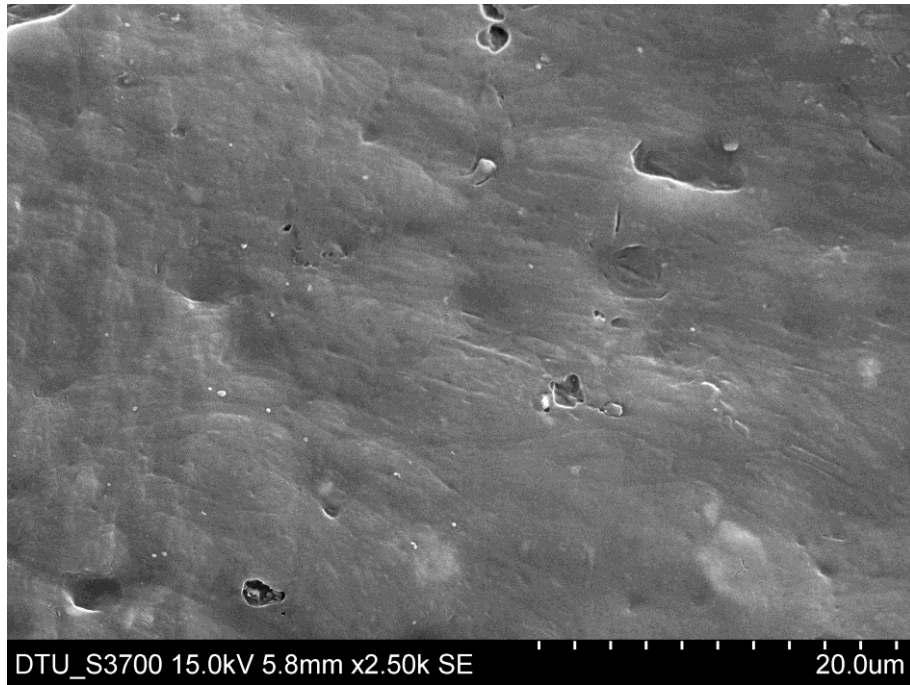Fig 27: SEM image of **ASM73** terpolymer coating

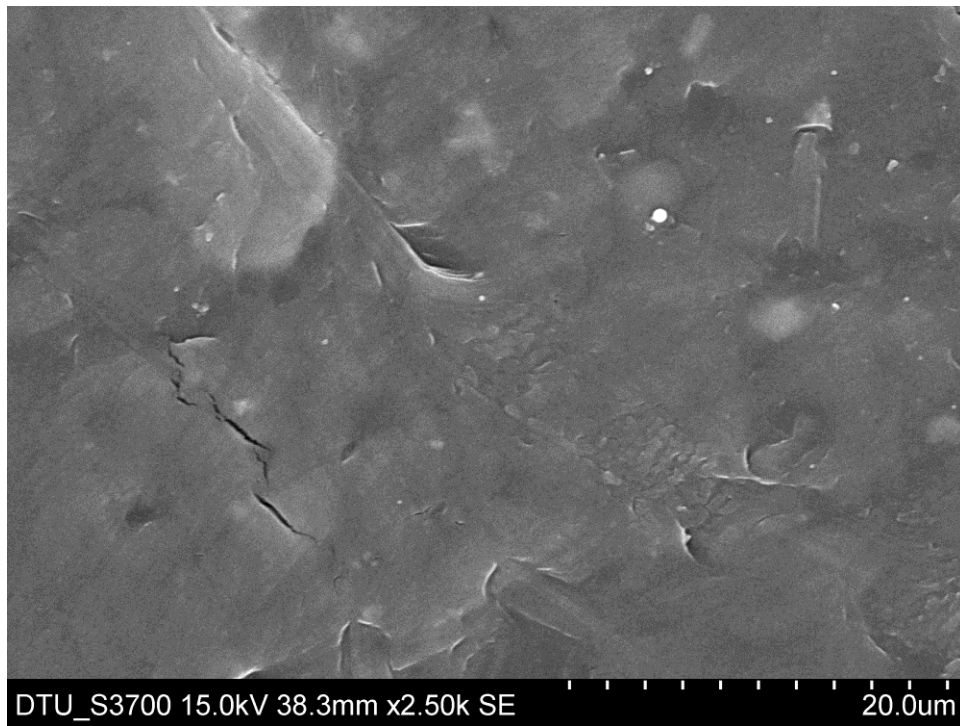Fig 28: SEM image of **ASM74** terpolymer coating

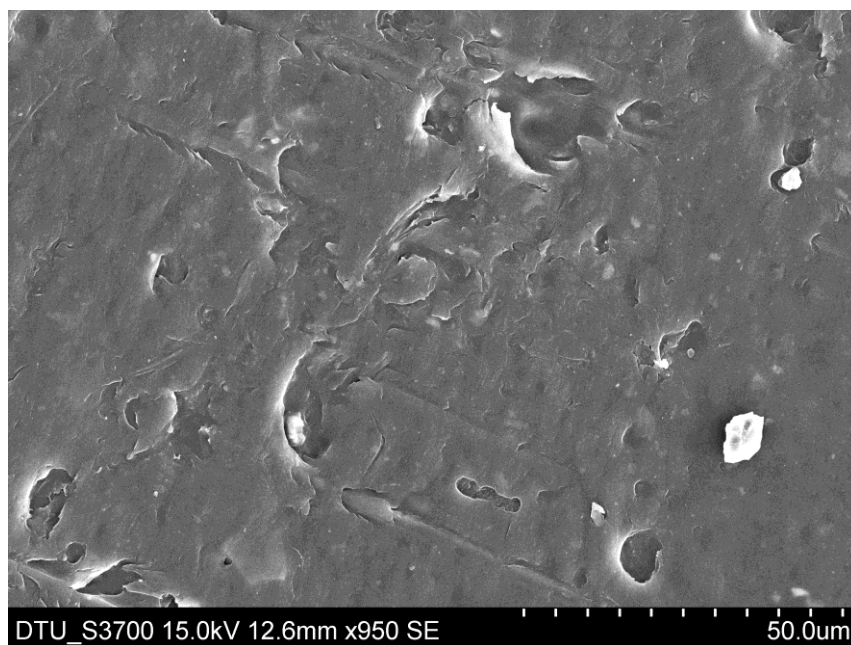Fig 29: SEM image of **ASM73 C** terpolymer composite coating

Fig 30: SEM image of **ASM74 C** terpolymer composite coating

The surfaces of the composite coatings were a bit less uniform and even than terpolymers. The particle of TiO_2 and Al_2O_3 were not visible at the surface. The surfaces of the terpolymers were free from cracks and holes. Only a few holes were present at the surface of the composites.

4.2.2 Thermal analysis

4.2.2.1 Differential scanning calorimetry (DSC)

DSC was performed for the thermal analysis of the terpolymers and the composites. The DSC curve of **PAA** shows that it was stable up to a temperature of around 120 °C (figure 31) and it was free of chemical and physical changes up to this temperature. The endothermic peak at 128.21 °C is due to the dehydration [5],[22] . There are two more peaks at 142 and 152 °C which probably represent the Tm of different segments. The absence of exothermic peaks in the curve implies that there was no oxidative thermal degradation. The DSC curves of the terpolymers and composite shows peaks in the same region as in that of **PAA**. The DSC curve of the **ASM52, ASM73, ASM74, ASM73 C** and **ASM74 C** are shown in figure 32 to 36.
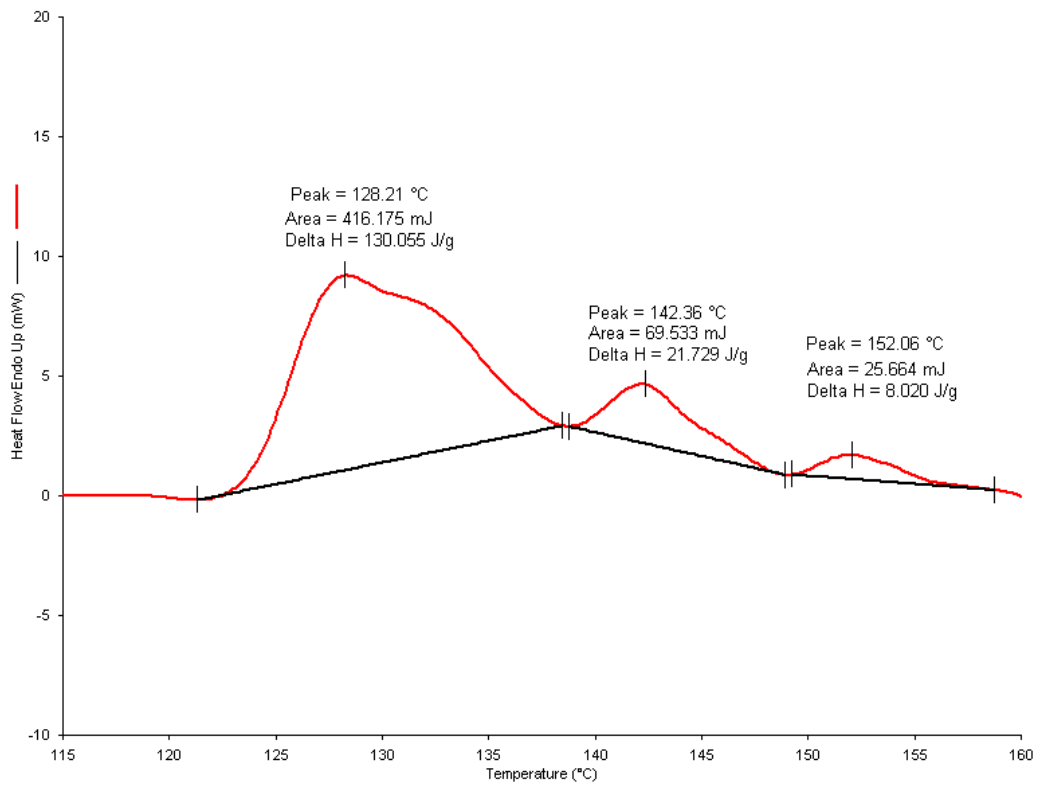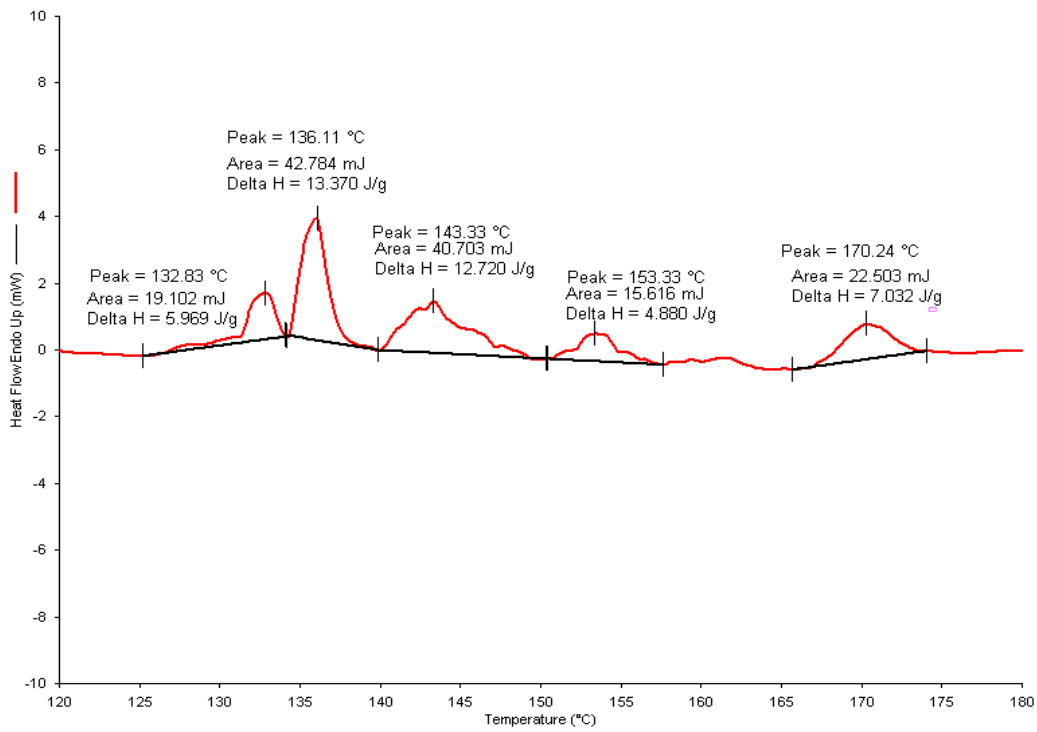
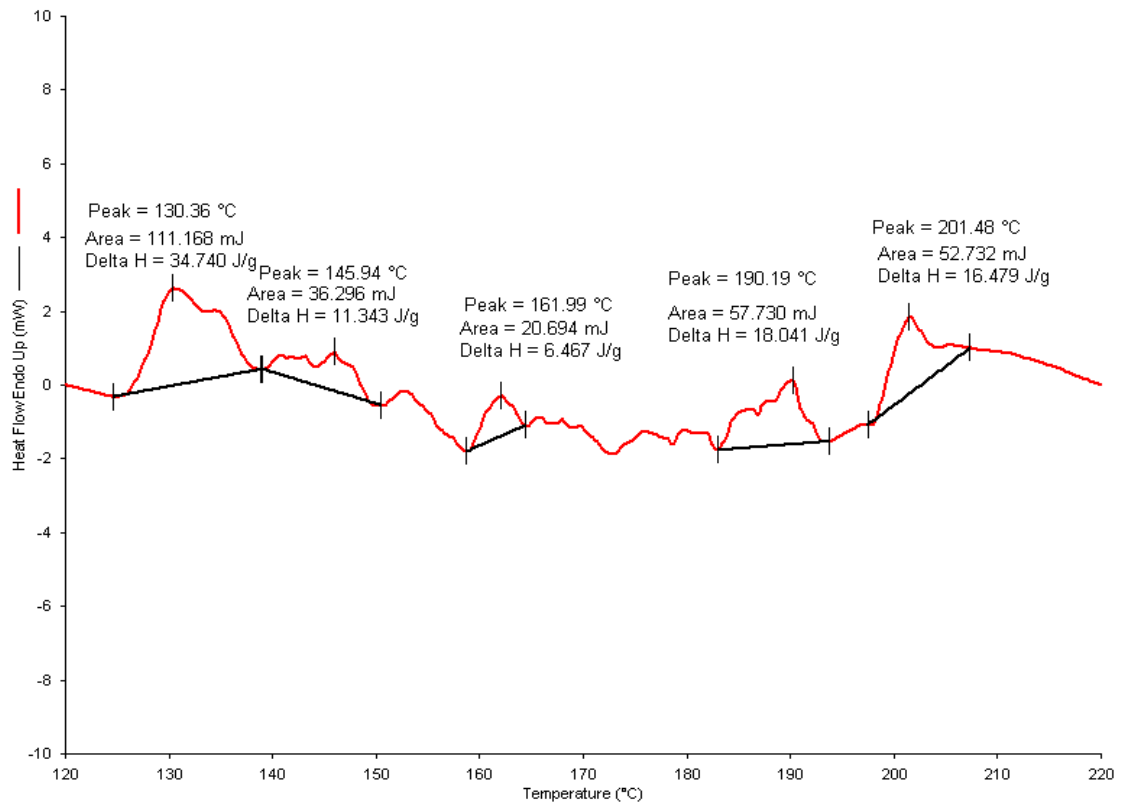Figure 31: DSC curve of **PAA**

Figure 32: DSC curve of **ASM52**
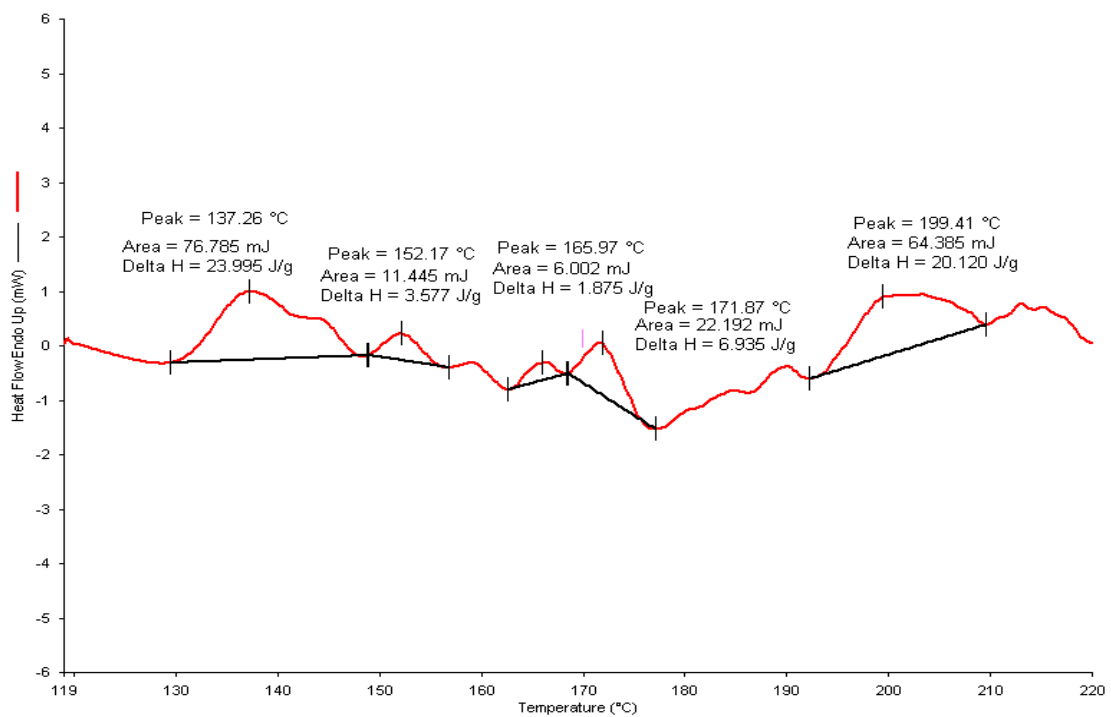
Figure 33: DSC curve of **ASM73**
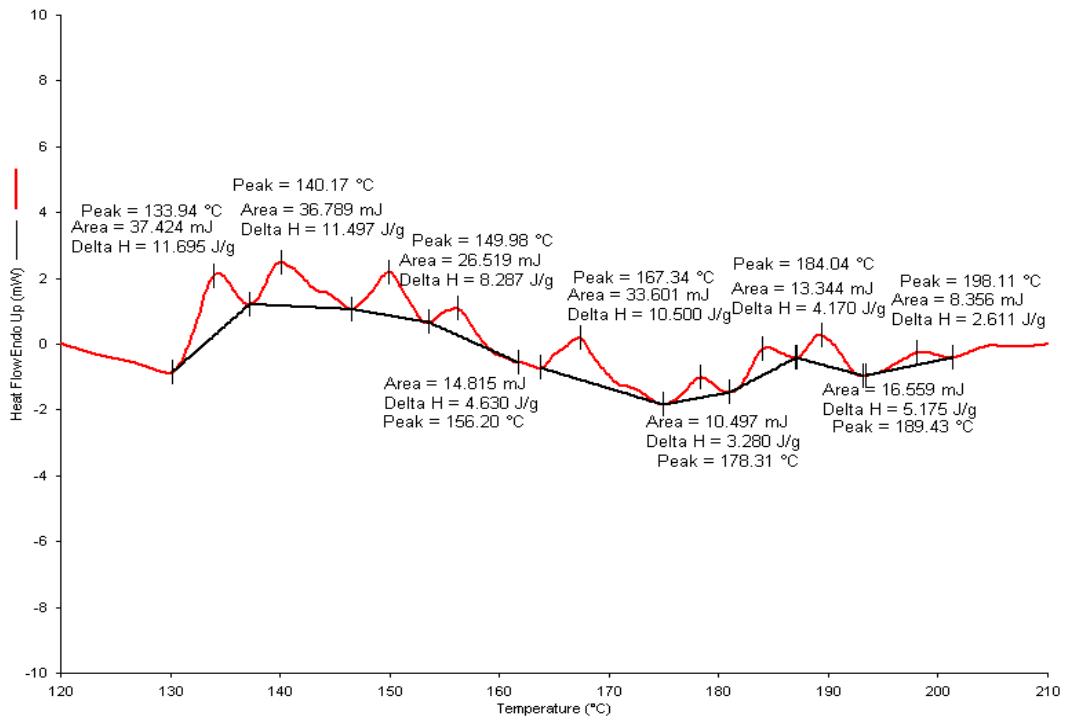

Figure 34: DSC curve of **ASM74**

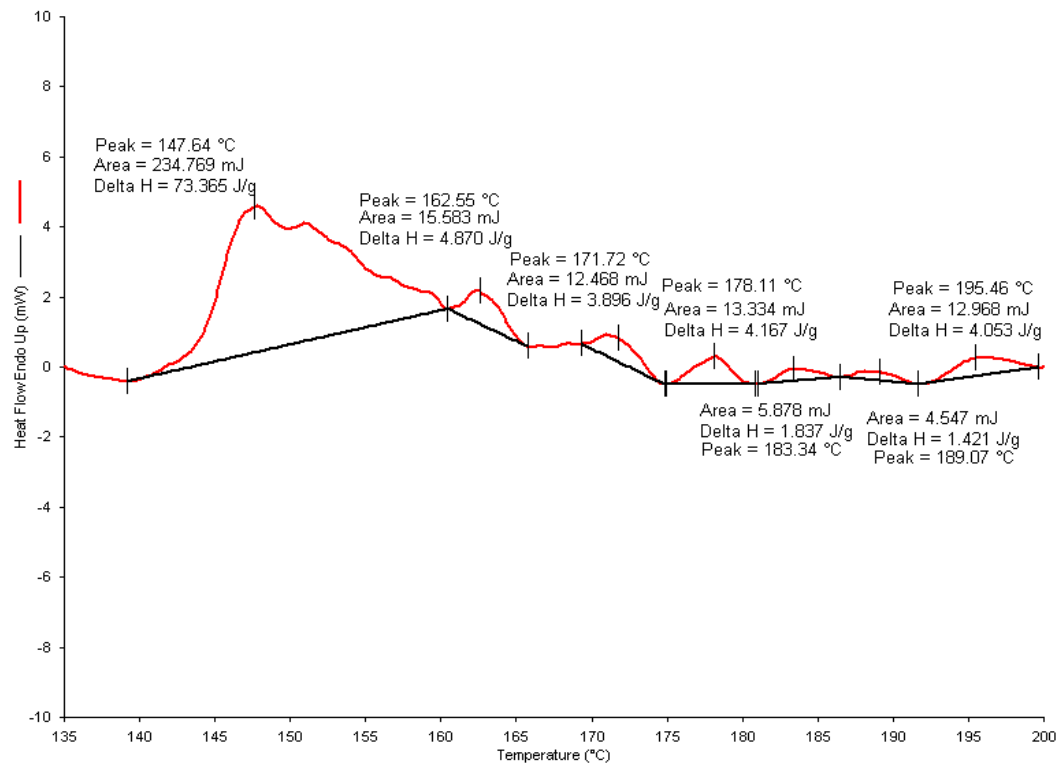Figure 35: DSC curve of **ASM73 C**

Figure 36: DSC curve of **ASM74 C**

In the DSC curve of the terpolymers and the composites, there are peaks at around 130, 142 and 152 °C, are in the same region as that in **PAA**, but some other peaks are also present at higher temperatures probably due to the melting of the different polymeric segments formed as a results of random arrangement of acrylic acid, styrene and maleic anhydride in the terpolymer. Also the thermal stability of the composite was higher than the terpolymers. **ASM74 C** showed maximum thermal stability up to a temperature of around 138 °C. it was completely free of chemical and physical changes up to this temperature.

4.2.3 Mechanical Testing

4.2.3.1 Flexural strength test

The flexural strength was carried out by using three point bending system. The results of the flexural strength showed that terpolymer coated glass possess better mechanical strength than the **PAA-G**. Also reinforcing the terpolymer with particulate reinforcements TiO_2 and Al_2O_3 resulted in an increase in the flexural strength of the terpolymer. The flexural strengths of glass, **PAA** coated glass, terpolymer coated glass and terpolymer composite coated glass samples are listed in table 4 and their graphs of load vs extension are shown in figure 37-44. The flexural data is represented by bar graph (figure 45).

Table 4: Flexural strength of samples

S.No	Sample	Flexural Strength (MPa)
1	Uncoated Glass	68.75
2	PAA-G	85.96
3	ASM52-G	86.95
4	ASM102-G	87.84
5	ASM73-G	96.20
6	ASM74-G	106.02
7	ASM73 C-G	146.20
8	ASM74 C-G	136.01

Starting from the glass without coating, it has flexural strength of 68.75 MPa, on the other hand the **ASM73 C-G** and **ASM74 C-G** possess significantly higher flexural strength of 146.00 and 136.01 MPa respectively and there was not much difference observed between the flexural strengths of these two composite coated samples. Between these two extremes, there are terpolymer coatings which have moderately high flexural strengths.
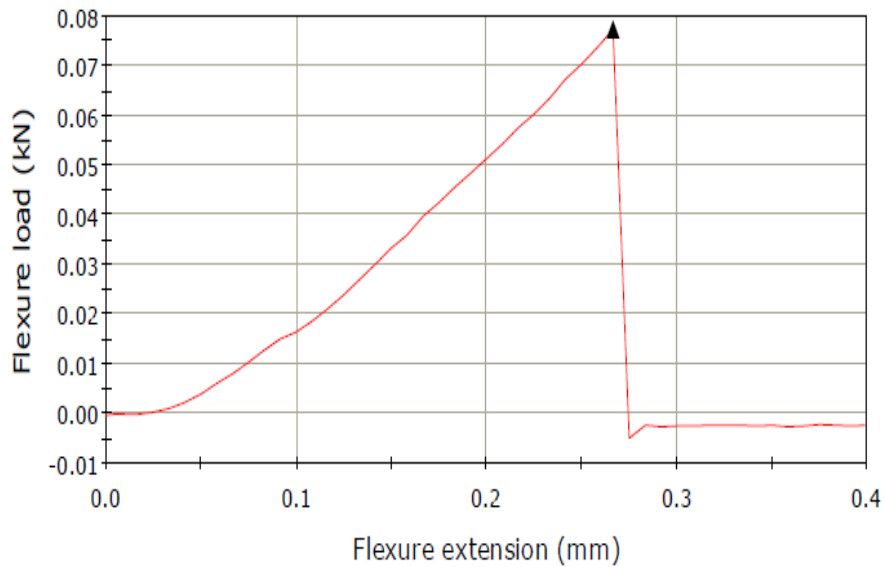
Fig 37: Flexural load vs flexural extension graph of uncoated glass.

Fig 38: flexural load vs flexural extension graph of **PAA-G**.

Fig 39: flexural load vs flexural extension graph of **ASM52-G.**
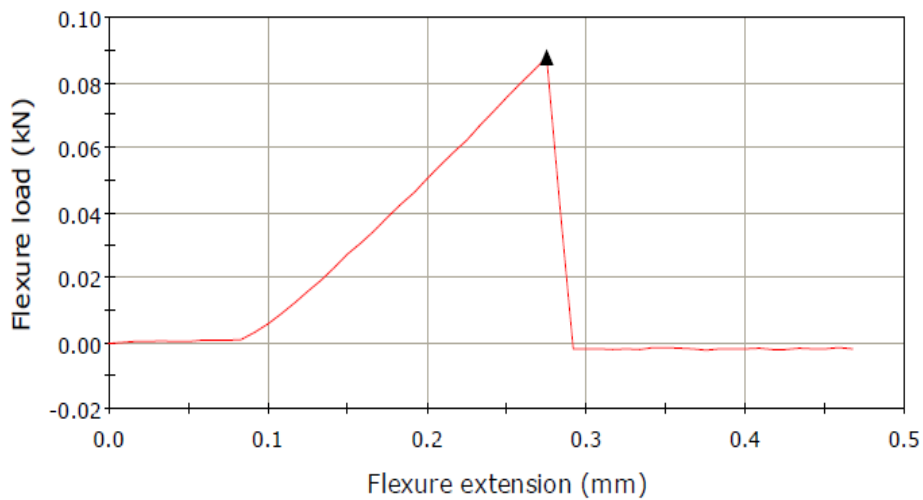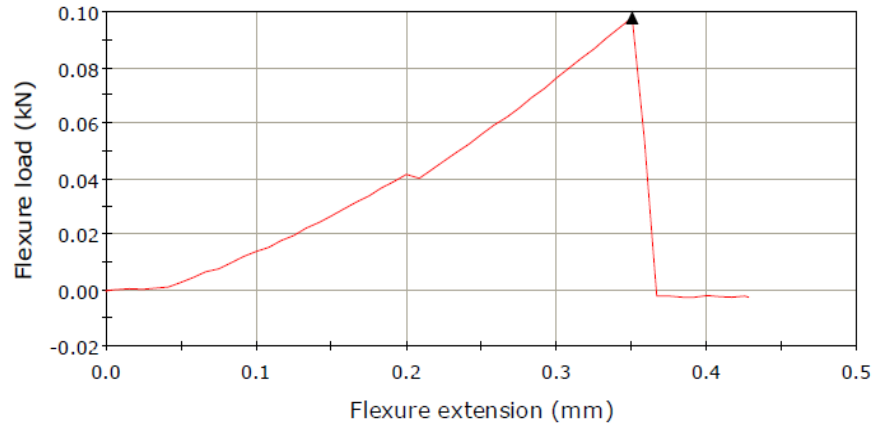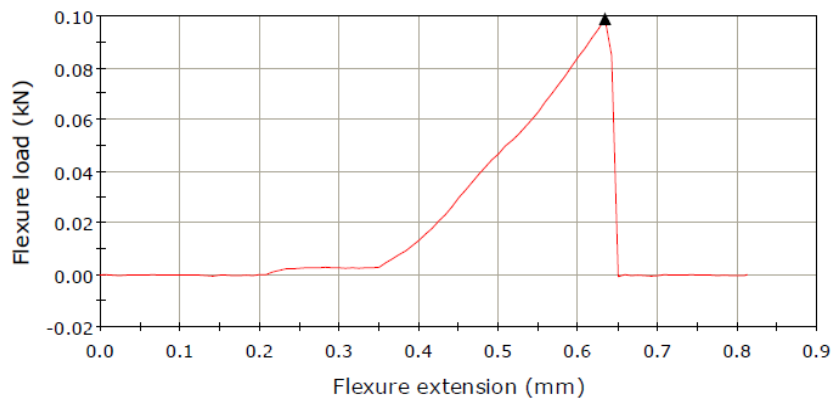

Fig 40: flexural load vs flexural extension graph of **ASM102-G.**
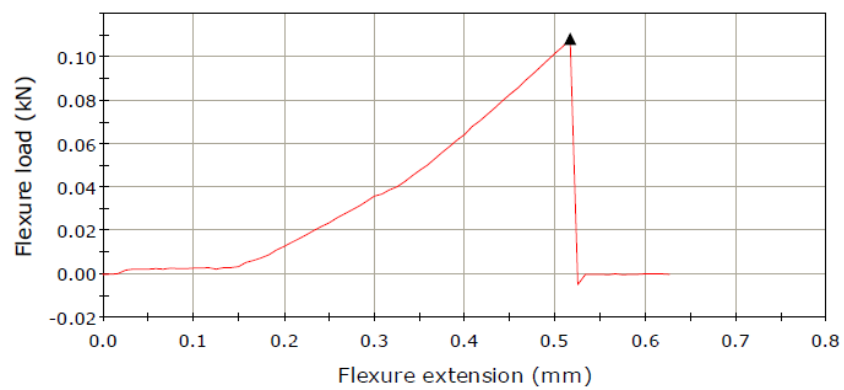

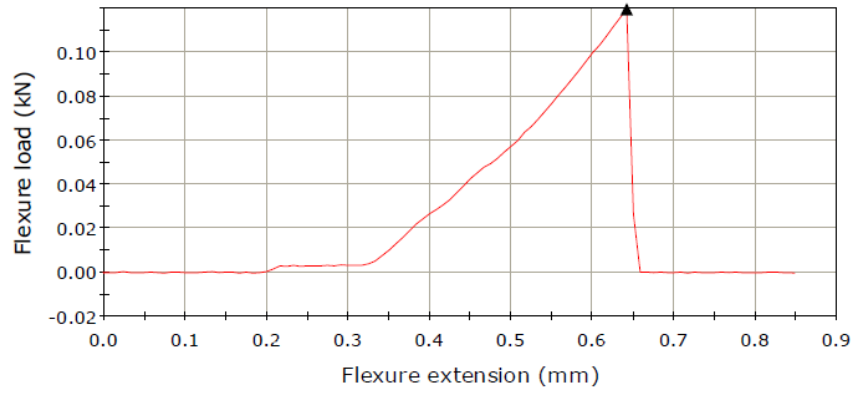Fig 41: flexural load vs flexural extension graph of **ASM73-G** sample.

Fig 42: flexural load vs flexural extension graph of **ASM74-G** sample.
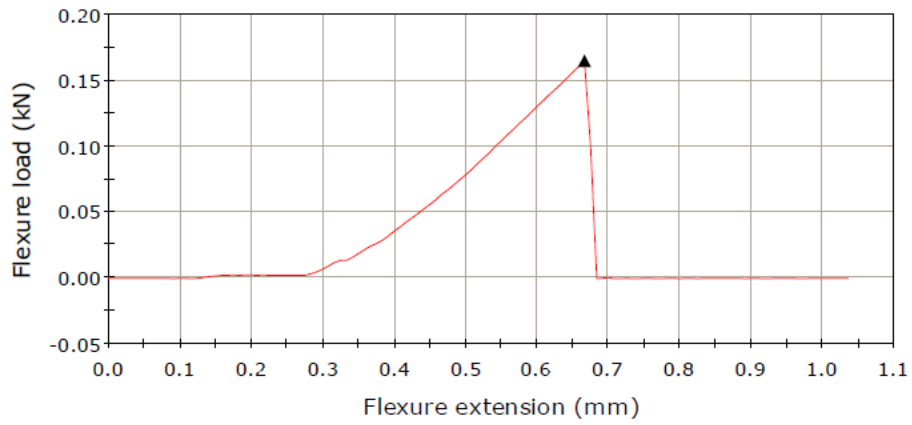

Fig 43: flexural load vs flexural extension graph of **ASM73 C-G** sample
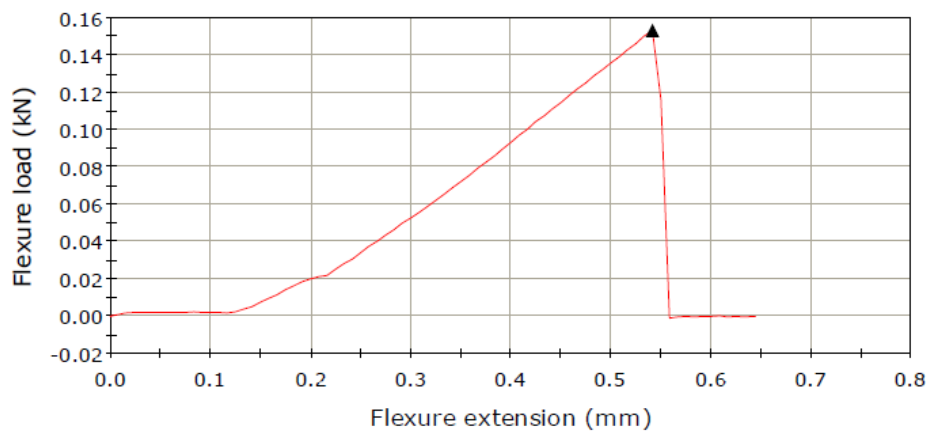
Fig 44: flexural load vs flexural extension graph of **ASM74 C-G** sample.
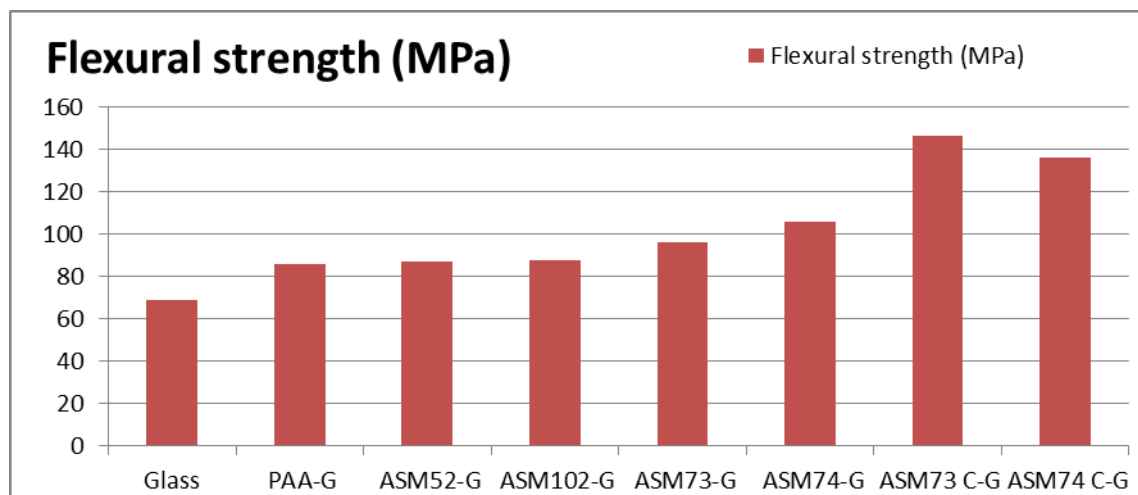
Figure 45: Graphical representation of Flexural data

Flexural strength test data showed that with increase in the percentage of styrene and maleic anhydride, there was an increase in the flexural strength of the terpolymer. It has been found that **ASM73 C-G** which contains 0.5 % TiO$_2$ and 0.25 % Al$_2$O$_3$ (by weight) possessed higher flexural strength but it lost its clarity also. So the composite **ASM74 C** was prepared with 0.25 % of both TiO$_2$ and Al$_2$O$_3$ (by weight). The **ASM74 C-G** showed flexural strength comparable to **ASM73 C-G** and it also maintained its clarity.

4.2.3.2 Izod impact test

The impact strength of glass is important factor for its applications. The Izod impact strength of glass and **PAA-G** was found to be 22.85 and 26.66 j/m respectively. The impact strengths of the terpolymer coated glass, **ASM73-G** and **ASM74-G** was found to be 30.53 and 33.33 j/m respectively which is higher than the glass and the **PAA-G**. The composites **ASM73 C-G** and **ASM74 C-G** registered the impact strengths 43.33 and 40 j/m respectively which is comparable to each other but remarkably higher than that of **PAA-G** and glass. The use of styrene and maleic anhydride with acrylic acid increased the impact strength of the terpolymer and the use of TiO$_2$-Al$_2$O$_3$ further enhanced it. The tables 5-10 represent the impact strength of terpolymers and composites. The figure 46 is graphical representation of impact test data.

Table 5: Impact strength of glass sample

Izod Impact strength as per (ASTM Standard):	j/m	kg.cm/cm	kg.m/m
	22.8571	2.33	2.33

Izod Impact strength as per (IS / ISO Standard):	j/mm^2	j/cm^2	kj/m^2
	0.0022	0.225	2.2497

Table 6: Impact strength of **PAA- G**

Izod Impact strength as per (ASTM Standard):	j/m	kg.cm/cm	kg.m/m
	26.6667	2.7183	2.7183

Izod Impact strength as per (IS / ISO Standard):	j/mm^2	j/cm^2	kj/m^2
	0.0021	0.21	2.0997

Table 7: Impact strength of **ASM73- G**

Izod Impact strength as per (ASTM Standard):	j/m	kg.cm/cm	kg.m/m
	30.5344	3.1126	3.1126

Izod Impact strength as per (IS / ISO Standard):	j/mm^2	j/cm^2	kj/m^2
	0.0025	0.2458	2.4585

Table 8: Impact strength of **ASM74-G**

Izod Impact strength as per (ASTM Standard):	j/m	kg.cm/cm	kg.m/m
	33.3333	3.3979	3.3979

Izod Impact strength as per (IS / ISO Standard):	j/mm^2	j/cm^2	kj/m^2
	0.0026	0.2625	2.6247

Table 9: Impact strength of **ASM73 C- G**

Izod Impact strength as per (ASTM Standard):	j/m	kg.cm/cm	kg.m/m
	43.3333	4.4173	4.4173

Izod Impact strength as per (IS / ISO Standard):	j/mm^2	j/cm^2	kj/m^2
	0.0034	0.3412	3.4121

Table 10: Impact strength of **ASM74 C-G**

Izod Impact strength as per (ASTM Standard):	j/m	kg.cm/cm	kg.m/m
	40	4.0775	4.0775
Izod Impact strength as per (IS / ISO Standard):	j/mm^2	j/cm^2	kj/m^2
	0.0031	0.315	3.1496
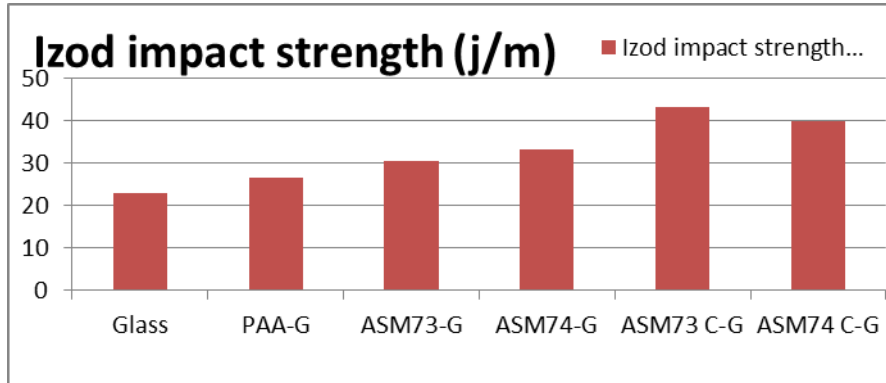
Figure 46: Graphical representation of Impact test data

Though the Impact Strength of **ASM73 C-G** was highest, but **ASM74 C-G** also showed remarkably higher impact strength than glass and PAA–G along with the maintenance of clarity.

Shattering Resistance

One more advantage of using terpolymer and composite coating is that the coating prevented the broken pieces from shattering into many pieces after impact. Shatter resistance is the ability of a material to hold the broken pieces of other brittle material after breakage. The terpolymer and composite coatings provided shatter resistance to the glass. The following figure 47 shows that the glass broke into many pieces but the terpolymer and composite coated glass broke into 2 pieces only after the application of flexural forces during flexural strength test.

A   B

C   D

E   F

Figure 47: (A) Broken sample of **ASM 73-G** under flexural forces (B) Broken sample of uncoated glass under flexural forces (c) Broken pieces of **ASM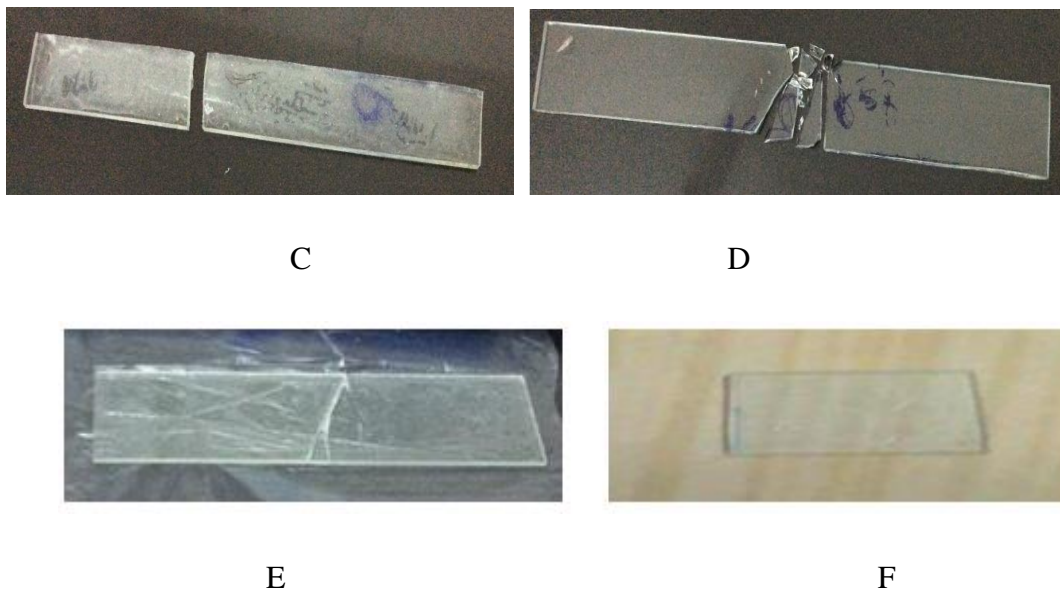73 C**-**G** under impact (d) Broken pieces of uncoated glass under impact (E) Broken sample of **ASM74-G** under flexural force (F) **ASM74 C-G**

The same effect was observed in the izod impact test. Here also the coating prevented the broken pieces of glass from shattering after breaking due to impact. From C and D images of figure 47, the difference between the clarity of **ASM73 C-G** and **ASM74 C-G** is clearly visible; **ASM74 C-G** possesses much better clarity than **ASM73 C-G.**

The flexural and the Izod impact test results showed that the use of styrene and maleic anhydride with acrylic acid resulted in an increase in the mechanical strength of the terpolymer coated glass. Reinforcing of the terpolymer **ASM73** and **ASM74** with TiO_2-Al_2O_3 further increased the mechanical strength of the terpolymer composite. The two composite coated glasses, **ASM73 C-G** and **ASM74 C-G** showed the comparable mechanical strength but much higher than glass and **PAA-G**. The **ASM73 C-G** gained little higher mechanical strength than **ASM74 C-G** but at the expense of clarity. **ASM74 C-G** showed much improved mechanical strength with clarity. Terpolymer and the composite both imparted shattering resistance to glass made it safer along with increasing the impact strength and flexural strength. On the basis of these results, we may propose that the remarkable increase in the mechanical strength of the composite sample is due to the interaction of polymer matrix with reinforcement which is also confirmed by FTIR.

CHAPTER 5   APPLICATIONS: FUTURE SCOPE

Polyacrylic acid has the potential to be used as a coating material for glass. Its properties can be modified by copolymerizing it with suitable comonomers. Use of styrene and maleic anhydride imparted strength, toughness and water resistance to the Poly(acrylic acid-styrene-maleic anhydride) terpolymer coating. Also the composite of the terpolymer with TiO_2-Al_2O_3 possesses better mechanical strength than the terpolymer. The clear terpolymer coatings can be used as protective coating for glass. Glass used for lightings, windows etc can be coated with the terpolymer.

The r composite gained much higher mechanical strength than terpolymer but their clarity is somewhat lesser than the terpolymers. TiO_2 is a white pigment so the terpolymer composite can be used for white colored protective coating for glass. This glass can be used for structural applications and translucent glass objects. At the same time transparency can be retained by using the appropriate amount of TiO_2 and Al_2O_3. Such glasses can be used where transparency is as important as mechanical strength. The improvement of the shatter resistance of glass by the terpolymer provides it an extra edge to be used as coating for glass objects of domestic use because of its safety. These terpolymer and composite coated glasses can be used for indoor and outdoor applications up to a temperature of around 130-135 °C.

CHAPTER 6   CONCLUSION

In present work, Terpolymers of acrylic acid with styrene and maleic anhydride were synthesized with different compositions using bulk polymerization technique: An effort has also been made to develop composite with TiO_2-Al_2O_3. Terpolymers **ASM52, ASM102, ASM73** and **ASM74** were synthesized and effect of the comonomers, styrene and maleic anhydride, on the properties of terpolymers was studied. The samples were characterized by FTIR and the IR spectra were found in accordance with the literature. SEM analysis of the terpolymer coatings showed that their surface were more even and uniform than the composite coatings. Because of high mechanical strength of terpolymers **ASM73** and **ASM74,** these were selected for preparation of composites, **ASM73 C** and **ASM74 C** with TiO_2-Al_2O_3. From DSC it is observed that i) the terpolymerization increased the thermal stability. ii) Also the composite exhibited higher thermal stability than terpolymers and **ASM74 C** was free from chemical and physical changes up to 138 °C. **ASM73 C** coated glass (**ASM73 C-G**) and **ASM74** coated glass (**ASM74 C-G**) showed significantly improved flexural strength of 146.20 and 136.01 MPa respectively which is much higher than **PAA-G** (polyacrylic acid coated glass) and uncoated glass. **ASM73 C-G** and **ASM74 C-G** also showed impact strength of 43.33and 40.00 j/m respectively, which is remarkably higher than that of glass and **PAA-G**. The **ASM74 C-G** showed significantly higher mechanical strength and its clarity was much better than **ASM73 C-G**. Another advantage of terpolymer/composite coatings is that it prevented the broken pieces of coated glass from shattering and thus makes the glass shatter resistant. On the basis of these results, we may propose that the remarkable increase in the mechanical strength of the terpolymer is due to use of styrene and maleic anhydride and reinforcement further increased the mechanical strength of composite due to the interaction of polymer matrix with reinforcement. Thus on the basis of present investigation we may conclude that **ASM73 C** and **ASM74 C** have potentiality to be used as protective coating material for glass.

References

1. http://www.toxipedia.org/display/toxipedia/Polyacrylic+Acid

2. http://www.sigmaaldrich.com/catalog/papers/23261730

3. Veljko Dragojlovic, Preparation of a Nonfogging Mirror: An Introductory Organic Chemistry Experiment Chem. Educator 13 (2008) 297–301.

4. Yun-ren Qiu, Lian-jun Mao, Wei-hua Wang, Removal of manganese from waste water by complexation−ultrafiltration using copolymer of maleic acid and acrylic acid, Trans. Nonferrous Met. Soc. China 2 (2014) 1196−1201.

5. J.L. de la Fuentea, M. Wilhelmb, H.W. Spiessc, E.L. Madrugad, M. Ferna´ndez-Garciad, M.L. Cerrada Thermal, morphological and rheological characterization of poly(acrylic acid-g-styrene) amphiphilic graft copolymers Polymer 46 (2005) 4544–4553.

6. L. Melo, R. Benavides, G. Martínez, L. Da Silva, M.M.S. Paula Degradation reactions during sulphonation of poly(styrene-co-acrylic acid) used as membranes Polymer Degradation and Stability (2014) 1-10.

7. Clemente Bretti , Francesco Crea , Carlos Rey-Castro , Silvio Sammartano Interaction of acrylic-maleic copolymers with H^+, Na^+, Mg^{2+} and Ca^{2+}: Thermodynamic parameters and their dependence on medium Reactive & Functional Polymers 65 (2005) 329–342.

8. Hatice Kaplan Can, Zakir MO Rzayev, Ali Güner H-Bonding Effect in Radical Terpolymerization of Maleic anhydride, Acrylic acid (Methyl acrylate) and Vinyl acetate Hacettepe J. Biol. & Chem. 40 (4) (2012) 427-443.

9. Inderjeet Kaur, Vandna Kumari, Bikram Singh Synthesis and Characterization of Acrylic acid Grafted Styrene- Maleic anhydride Copolymer Der Chemica Sinica, 3(2) (2012) 343-358.

10. James G. Kopchick , Robson F. Storey, Frederick L. Beyer, Kenneth A. Mauritz Poly[acrylic acid-b-styrene-b-isobutylene-b-styrene-b-acrylic acid] pentablock terpolymers: 1. Morphological characterization Polymer 48 (2007) 3739-3748.

11. Behnaz Hojjati, Ruohong Sui, Paul A. Charpentier Synthesis of TiO_2/PAA nanocomposite by RAFT polymerization Polymer Polymer 48 (2007) 5850-5858.

12. H.A. Ali, A.A. Iliadis Thin ZnO nanocomposite poly(styrene–acrylic acid) films on Si and SiO_2 surfaces Thin Solid Films 471 (2005) 154– 158.

13. Zhexiong Tang, Neil Alvarez, Sze Yang Organic / Inorganic Hybrid Material for Coating on Metals Mat. Res. Soc. Symp. Proc. 73 (2003) 57.1-57.7.

14. E. De Giglio & S. Cometa & N. Cioffi & L. Torsi & L. Sabbatini Analytical investigations of poly(acrylic acid) coatings electrodeposited on titanium-based implants: a versatile approach to biocompatibility enhancement Anal Bioanal Chem 389 (2007) 2055–2063.

15. J. Godnjaveca, J. Zabreta, B. Znoja, S. Skale, N. Veronovski, P. Venturini Investigation of surface modification of rutile TiO2 nanoparticles with SiO_2/Al_2O_3 on the properties of polyacrylic composite coating Progress in Organic Coatings 77 (2014) 47– 52.

16. Y. Xu a, L. Zhuang, H. Lin, H. Shen, J.W. Li Preparation and characterization of polyacrylic acid coated magnetite nanoparticles functionalized with amino acids Thin Solid Films 544 (2013) 368–373.

17. Wen-Cheng Chena, Chien-Ping Jub, Jen-Chyan Wanga, Chun-Cheng Hunga, Jiin-Huey Chern Lin Brittle and ductile adjustable cement derived from calcium phosphate cement/polyacrylic acid composites dental materials 24 (2008) 1616–1622.

18. http://micron.ucr.edu/public/manuals/EDS-intro.pdf

19. I. Oja, A. Mere, M. Krunks , C-H. Solterbeck , M. Es-Souni Properties of TiO_2 Films Prepared by the Spray Pyrolysis Method Solid State Phenomena 99-100 (2004) 259-264.

20. M. Burgos, M. Langlet Thin Solid Films 349 (1999) 19.

21. O. Harizanov, A. Harizanova Sol. Energy Mat. and Solar Cells 63 (2000) 185.

22. Stanislav Dubinska, Gideon S. Grader, Gennady E. Shter, Michael S. Silverstein, Thermal degradation of poly(acrylic acid) containing copper nitrate Polymer Degradation and Stability 86 (2004) 171-178.